The N-Terminal Domain of the Escherichia coli PriA Helicase Contains Both the DNA- and Nucleotide-Binding Sites. Energetics of Domain-DNA Interactions and Allosteric Effect of the...

ARTICLE *in* BIOCHEMISTRY · SEPTEMBER 2011

Impact Factor: 3.02 · DOI: 10.1021/bi201100k · Source: PubMed

Published in final edited form as:
Biochemistry. 2011 November 1; 50(43): 9167–9183. doi:10.1021/bi201100k.

The N-Terminal Domain of the *E. coli* PriA Helicase Contains Both the DNA- and the Nucleotide-Binding Sites. Energetics of Domain-DNA Interactions and Allosteric Effect of the Nucleotide Cofactors§

Michal R. Szymanski, **Paul J. Bujalowski**, **Maria J. Jezewska**, **Aleksandra M. Gmyrek**, and **Wlodzimierz Bujalowski***
Department of Biochemistry and Molecular Biology, Department of Obstetrics and Gynecology, The Sealy Center for Structural Biology, Sealy Center for Cancer Cell Biology, The University of Texas Medical Branch at Galveston, 301 University Boulevard, Galveston, Texas 77555-1053

Abstract

Functional interactions of the *E. coli* PriA helicase 181N-terminal domain with the DNA and nucleotide cofactors have been quantitatively examined. The isolated 181N-terminal domain forms a stable dimer in solution, most probably reflecting the involvement of the domain in specific cooperative interactions of the intact PriA protein - dsDNA complex. Only one monomer of the domain dimer binds the DNA, *i.e*., the dimer has one effective DNA-binding site. Although the total site-size of the dimer - ssDNA complex is ~13 nucleotides, the DNA-binding subsite engages in direct interactions ~5 nucleotides. A small number of interacting nucleotides indicates that the DNA-binding subsites of the PriA helicase, *i.e*., the strong subsite on the helicase domain and the weak subsite on the N-terminal domain, are spatially separated in the intact enzyme. Contrary to current views, the subsite has only a slight preference for the 3′-end OH group of the ssDNA and lacks any significant base specificity, although it has a significant dsDNA affinity. Unlike the intact helicase, the DNA-binding subsite of the isolated domain is in an open conformation, indicating the presence of the direct helicase domain - N-terminal domain interactions. The discovery that the 181N-terminal domain possesses a nucleotide-binding site places the allosteric, weak nucleotide-binding site of the intact PriA on the N-terminal domain. The specific ADP effect on the domain DNA-binding subsite indicates that in the intact helicase, the bound ADP not only opens the DNA-binding subsite but also increases its intrinsic DNA affinity.

Keywords

PriA protein; PriA N-terminal domain; Fluorescence Titrations; Protein - Nucleic Acid Interactions; Nucleotide Binding

The *E. coli* PriA helicase plays a fundamental role in the initiation of the ordered assembly of the primosome, a multi-protein complex that translocates on the DNA and catalyzes the priming reaction during the replication process (1–14). Formation of the primosome was originally discovered in phage replication systems (1–3,5,11). Further studies have shown

§This work was supported by NIH Grants GM46679 and GM58565 (to W. B.).

*Send Correspondence: Dr. W. M. Bujalowski, Department of Biochemistry and Molecular Biology, The University of Texas Medical Branch at Galveston, 301 University Boulevard, Galveston, Texas 77555-1053, Tel: (409) 772-5634, Fax: (409) 772-1790, wbujalow@utmb.edu.

that the primosome complex is assembled in recombination and repair processes of the *E. coli* chromosomal DNA, as a major event that initiates the restart of the stalled replication fork at the damaged DNA sites (6,12,13). The commencement of the primosome assembly occurs through the recognition of the damaged DNA site structure/sequence by the PriA protein, although the nature of this recognition reaction is not yet understood (4,5,9–11,13). The native PriA protein is a monomer with a molecular mass of 81.7-kDa (1,2,5,15–17). The tertiary structure of the monomer contains two functional domains, the helicase domain encompassing ~540 amino acid residues from the C-terminus and the N-terminal domain, which comprises the ~181 amino acid residues (181N terminal domain) from the N-terminus (14,18).

Activities of the PriA protein *in vivo* are related to the ability of the enzyme to interact with both the ss and the dsDNA (1–12,15–17,19–22). Quantitative thermodynamic analyses showed that in the complex with the ssDNA, the total DNA-binding site of the PriA helicase occludes ~20 nucleotides of the nucleic acid (15–17,19–22). Within the total DNA-binding site, the protein possesses a strong ssDNA-binding subsite, located on the helicase domain in the central part of the enzyme molecule, which engages in interactions with only ~6 nucleotides (15–17,19–22). In the complexes with the dsDNA, as well as in the ssDNA gap recognition reaction, the enzyme engages the nucleic acid exclusively using the strong DNA-binding subsite on the helicase domain (19,22). As a result, the total site-size of the PriA - dsDNA complex is only ~5 base pairs, while the enzyme preferentially recognizes the ssDNA gap containing 5 nucleotides (19,22).

During the dsDNA unwinding reaction, the binding and/or hydrolysis of NTPs regulate the PriA activity, including the affinity toward different conformations of the DNA (2,5,11,15–17,19–22). The characteristic feature of the PriA protein, so far not found in other monomeric helicases, is that the enzyme possesses not one but two nucleotide-binding sites, a strong and a weak site, which profoundly differ in their affinities for the type of cofactors and the effects on the intrinsic affinity of the protein - DNA complexes (19,20,21–23). Moreover, cooperative interactions between the two nucleotide-binding sites indicate communication between them. Another peculiar aspect of the PriA helicase is that saturation of both nucleotide-binding sites, specifically with ADP, induces the engagement of the N-terminal domain in interactions with the DNA (21). This conclusion was reinforced by the fact that the ssDNA-binding activity of the isolated 181N-terminal domain has been detected (14). Thus the enzyme possesses two DNA-binding subsites, one located on the helicase domain and the other on the N-terminal domain. The intricate, structure-function organizations of the PriA helicase - ssDNA - nucleotide complexes, based on these studies, are schematically depicted in Figure 1a (15–17,20,21).

Understanding the PriA helicase interactions with the DNA absolutely requires the elucidation of the functional role of its DNA-binding subsites and the effect of the nucleotide cofactor on both subsites (15–17,19–23). Although the strong subsite - DNA interactions have been intensively examined, analogous interactions of the subsite located on the N-terminal domain are much less understood (14,18). The crystal structures of the truncated N-terminal domain containing 105 amino acid residues (105N terminal subdomain) have been solved at 2.5 Å resolution (Figure 1b) (18). The protein forms a dimer where two monomers interact through their N-terminal fragments (intervening dimer). The 105N-terminal subdomain retains its ssDNA-binding activity in solution (18). Nevertheless, quantitative analyses of interactions of the 105N-terminal subdomain and the complete 181N-terminal domain with the ssDNA have not been addressed and available qualitative analyses provide confusing results (see below). Nothing is known about the stoichiometries and intrinsic energetics of the complete 181N-terminal domain - ssDNA/dsDNA complexes. Whether or not one of the PriA nucleotide-binding sites is located on the

domain is unknown. The role of the cofactors and the structure of their phosphate groups in the N-terminal domain - nucleic acid association, if any, have never been addressed.

In this communication, we describe quantitative studies of the interactions of the 181N-terminal domain of the PriA helicase with the ss and dsDNA, and the effect of the nucleotide cofactors on the recognition process. The domain forms a dimer, which may reflect its involvement in the intact enzyme cooperative interactions. Only one monomer of the dimer binds the ssDNA, engaging in direct interactions with 5 ± 1 nucleotides. The DNA-binding subsite of the isolated domain is in open conformation and has only a modest preference for the 3′-end of the nucleic acid. We discovered that the 181N-terminal domain possesses a nucleotide-binding site, which corresponds to the weak nucleotide-binding site of the intact PriA helicase.

MATERIALS & METHODS

Reagents and Buffers

All solutions were made with distilled and deionized >18 MΩ (Milli-Q Plus) water. All chemicals were reagent grade. Buffer C is 10 mM sodium cacodylate adjusted to pH 7.0 with HCl, 1 mM DTT, 20 mM NaCl, 5 mM $MgCl_2$, and 25% glycerol (w/v) (15–17,19–23).

The 181N-Terminal Domain of the PriA Protein

The fragment of the *E. coli* PriA protein gene coding 181 amino acid residues from the N-terminus with C-terminal His-Tag has been placed under the T7 promoter in plasmid Pet30a. The domain has been purified using the standard Ni-Sepharose, High-Performance column (Piscataway, NJ). Subsequently, the sample was passed through the heparin column at 300 mM NaCl (50 mM Tris/HCl pH 7.5, 10% (w/v) glycerol, 1 mM DTT), followed by elution through the DEAE cellulose column at 150 mM NaCl (50 mM Tris/HCl pH 7.5, 10% (w/v) glycerol, 1 mM DTT). The protein was > 99% pure as judged by polyacrylamide electrophoresis with Coomassie Brilliant Blue staining. The tagged domain has DNA-binding properties indistinguishable for the unmodified protein (data not shown) (14,18). The protein concentration was spectrophotometrically determined, with the extinction coefficient $\varepsilon_{280} = 6.946 \times 10^4\ cm^{-1}M^{-1}$ (dimer) obtained using an approach based on the Edelhoch's method (24,25).

Nucleotides and Nucleic Acids

ATPγS and ADP were from Sigma (Saint Louis, Mi). TNP-ADP was from Invitrogen (Eugene, OR). Unmodified nucleic acid oligomers were purchased from Midland Certified Reagents (Midland, TX). Nucleic acids were at least >95% pure as judged by electrophoresis on polyacrylamide gels. The dsDNA substrate was obtained by mixing the ssDNA oligomer, ACGAGCCTGC, with the complementary oligomer, warming the mixture for 5 minutes at 95°C, and slowly cooling for a period of ~3 – 4 hours (19,22). The integrity of the dsDNA substrate has been checked by UV melting and analytical ultracentrifugation techniques (19,22,26,27). The melting temperature of the examined dsDNA oligomer is >54°C in the studied solution conditions. The etheno-derivatives of adenosine oligomers were obtained by modification with chloroacetaldehyde (15–17,19,21,23,28–31). This modification goes to completion and provides a fluorescent derivative of the nucleic acid. The concentrations of the etheno-derivative of the nucleic acids were determined using the extinction coefficient, $\varepsilon_{257} = 3700\ cm^{-1}M^{-1}$ (nucleotide) (15–17,28).

Fluorescence Measurements

All steady-state fluorescence titrations were performed using the ISS PC-1 spectrofluorometer (Urbana, IL) as previously described by us (15–17,19–23,32–36). The

181N-terminal domain binding was followed by monitoring the etheno-derivative fluorescence of the nucleic acids (λ_{ex} = 325 nm, λ_{em} = 410 nm). Binding of TNP-ADP to the domain was examined using the quenching of the protein fluorescence induced by the cofactor (λ_{ex} = 300 nm, λ_{em} = 345 nm) (32–36). Computer fits were performed with Mathematica (Wolfram, IL) and KaleidaGraph (Synergy Software, PA). The relative fluorescence increase, ΔF, of the DNA emission upon protein binding is defined as $\Delta F = (F_i - F_o)/F_o$, where F_i is the fluorescence of the sample at a given titration point "i" and F_o is the initial fluorescence of the same solution, corrected for the background (15–17,19–23,32–38). Analogously, the relative fluorescence quenching is defined as, $\Delta F = (F_o - F_i)/F_o$ (32–38). In the case of titrations with the nucleotide analog, TNP-ADP, the fluorescence intensity of the sample, F_i, was corrected for the dilution and inner filter effect as (20,21,23)

$$F_i=(F_{ie} - B_i)\left(\frac{V_i}{V_o}\right)10^{0.5b(A_{i,lex}+A_{i,lem})} \quad (1)$$

where F_{ie} is the experimentally measured fluorescence intensity, B_i is the background, V_i is the volume of the sample at a given titration point, V_o is the initial volume of the sample, b is the total length of the optical path in the cuvette expressed in cm, $A_{i\lambda ex}$ and $A_{i\lambda em}$ are the absorbances of the sample at excitation and emission wavelengths, respectively.

Quantitative Analysis of the Fluorescence Titration Curves of the 181N-Terminal Domain - DNA Associations or the Nucleotide Binding to the Domain

Quantitative estimates of the total average degree of binding, $\Sigma\Theta_i$ (average number of bound ligand molecules per macromolecule) and the free ligand concentration, L_F, independent of any assumption about the relationship between the observed spectroscopic signal, ΔF, and $\Sigma\Theta_i$ was accomplished using a quantitative approach previously described by us (15–17,19–23,32–38).

Analytical Ultracentrifugation Measurements

Analytical ultracentrifugation experiments were performed with an Optima XL-A analytical ultracentrifuge (Beckman Inc., Palo Alto, CA), as previously described by us (20,31,40–44). Sedimentation equilibrium scans were collected at the absorption band of the protein (280 nm). The sedimentation was considered to be at equilibrium when consecutive scans, separated by time intervals of 8 hrs, did not indicate any changes. For the n-component system, the total concentration at radial position r, c_r, is defined by (45)

$$c_r=\sum_{i=1}^{n} c_{b\,i}\exp\left[\frac{(1-\bar{\nu}_i\rho)\omega^2 M_i(r^2-r_b^2)}{2RT}\right]+b \quad (2)$$

where c_{bi}, $\bar{\nu}_i$, and Mi are the concentration at the bottom of the cell, partial specific volume and molecular weight of "i" component, respectively, ρ is the density of the solution, ω is the angular velocity, and b is the base-line error term. Equilibrium sedimentation profiles were fitted to eq. 2 with M_i and b as fitting parameters (20,31,40–44).

Photo-Cross-Linking Experiments

Photo-cross-linking of the 181N-terminal domain - ssDNA complex has been performed in the same buffer as the binding experiments. The ssDNA oligomer, $dT(pT)_{19}$, has been labeled at the 5′ end with [^{32}P], using polynucleotide kinase (19,31,46,47,48). The samples

(total volume 40 μl) were placed on Parafilm, immersed in a 10°C water bath, and irradiated for 20 minutes, at a distance of 11 cm, using a mineral lamp (model UVG-11) with a maximum output of 254 nm. The controls were performed to determine the optimal time for cross-linking and to avoid possible degradation of the protein by prolonged exposure to UV light. The samples collected at different protein concentrations were loaded on 15% SDS polyacrylamide gel and electrophoresis was performed at a constant voltage. The gels were stained with Coomassie Brilliant Blue and scanned, using the phosphorimager SI (Molecular Dynamics, PA) (19,31,47,48).

RESULTS

The Oligomeric State of the PriA 181N-Terminal Domain in Solution

The primary structure of the 181N-terminal domain of the PriA helicase indicates that the molecular mass of the monomer is ~21,000 kDa. The oligomeric state of the protein in solution has been addressed using the analytical ultracentrifugation method (20,31,40–44). An example of the sedimentation equilibrium profile of the 181N-terminal domain recorded at the protein absorption band (280 nm) is shown in Figure 2. The protein concentration is 5.98×10^{-6} M (monomer). The solid line is the nonlinear least-squares fit, using the single exponential function defined by eq. 2. The fit provides an excellent description of the experimental curve, indicating the presence of a single species with the molecular weight of 41,000 ± 3000. Adding additional exponents does not improve the statistics of the fit (data not shown). The equilibrium sedimentation experiments have been performed at different protein concentrations and different rotational speeds, providing the molecular weight ranging between ~39,000 – 42,000 (data not shown). These results indicate that, similar to the truncated 105N-terminal domain, the 181N-terminal domain exists as a dimer in solution in the protein concentration range studied in this work (18) (see Discussion).

Binding of the 181N-Terminal Domain To the ssDNA Oligomers. Maximum Stoichiometries of the Formed Complexes

In the course of our studies, we have found that formation of the 181N-terminal domain complex with the etheno-derivatives of the homo-adenosine polymer and oligomers causes a strong increase of the nucleic acid fluorescence, providing an excellent signal to perform high-resolution measurements of the protein - ssDNA complex formation (Materials & Methods). The fundamental problem of the stoichiometry of the domain - ssDNA complex, as well as the functional structure of the nucleic acid binding site has been addressed using a series of ssDNA oligomers with different numbers of nucleotides (15–17,21,22,31). Similar strategies have been applied in our previous studies of different protein - nucleic acid systems including the intact PriA helicase (15–17,21,22,31,49,50). The use of the ssDNA oligomers is also dictated by the fact that the domain - polymer ssDNA complex precipitates at higher protein concentrations (data not shown).

Fluorescence titrations of the ssDNA 12-mer, dεA(pεA)$_{11}$, with the 181N-terminal domain at three different nucleic acid concentrations, in buffer C (pH 7.0, 10°C), are shown in Figure 3a. The concentration of the domain is expressed as dimer. The shift of the titration curve at a higher nucleic acid concentration, results from the fact that more protein is required to obtain the same total average degree of binding, $\Sigma\Theta_i$ (31–36). The selected nucleic acid concentrations provide separation of the titration curves up to the relative fluorescence increase of ~1.5. The values of $\Sigma\Theta_i$ have been obtained using the quantitative approach outlined in Materials & Methods (31–36). Figure 3b shows the dependence of the relative fluorescence increase of the nucleic acid, ΔF, as a function of $\Sigma\Theta_i$ of the domain. Extrapolation to the maximum fluorescence change, $\Delta F_{max} = 2.55 \pm 0.11$, provides the

stoichiometry of the complex 0.98 ± 0.09. Thus, a single 181N-terminal domain dimer binds to the ssDNA 12-mer.

Analogous fluorescence titrations of the 24-mer, dεA(pεA)$_{23}$, at three different nucleic acid concentrations, are shown in Figure 3c. The maximum increase of the nucleic acid fluorescence at saturation is significantly lower than that observed for the 12-mer, reaching the value of ~ 1.4 (see Discussion). The dependence of the relative fluorescence increase of the nucleic acid, ΔF, as a function of $\Sigma\Theta_i$ is shown in Figure 3d. Extrapolation to the maximum fluorescence change, ΔF_{max} = 1.41 ± 0.08, provides the stoichiometry of the complex 0.91 ± 0.09. Thus, in spite of the fact that the oligomer is twice as long as the 12-mer, only a single 181N-terminal domain dimer binds to the ssDNA 24-mer.

On the other hand, increasing the length of the ssDNA oligomer only by 2 nucleotides changes the maximum stoichiometry of the 181N-terminal domain - ssDNA complex. Fluorescence titrations of the 26-mer, dεA(pεA)$_{25}$, with the domain at three different oligomer concentrations, are shown in Figure 4a. The dependence of the relative fluorescence increase of the 26-mer, as a function of $\Sigma\Theta_i$ of the 181N-terminal domain on the oligomer, is shown in Figure 4b. The plot is clearly nonlinear, indicating the presence of two binding phases (31–36,49,50). Extrapolation of the second affinity phase to the maximum fluorescence increase ΔF_{max} = 1.6 ± 0.08 provides $\Sigma\Theta_i$ = 2.2 ± 0.2. Thus, the 26-mer provides enough interaction space for the binding of two dimers of the 181N-terminal domain.

Number of Nucleotides Directly Engaged in Interactions with the 181N-Terminal Domain Dimer

Analogous quantitative analysis of the maximum stoichiometry of 181N-terminal - ssDNA complexes, as described above, has been performed for an entire series of ssDNA oligomers. The dependence of the maximum number of the bound domain dimers per ssDNA oligomer upon the length of the oligomer is shown in Figure 5. The selected ssDNA oligomers range from 8 to 33 nucleotides in length. A single 181N-terminal dimer binds to the oligomers containing 8, 10, 12, 14, 16, 18, 20, and 24 nucleotides. Sharp transition from a single dimer, bound per ssDNA oligomer, to two dimers, bound per oligomer, occurs between 24- and 26-mers (Figure 5). However, a further increase in the length of the oligomer, up to 33 nucleotides, does not lead to the increase of the number of the bound domain dimers. These data indicate that a total site-size of the 181N-terminal domain dimer - ssDNA complex encompasses a minimum of 13 ± 1 nucleotides per protein dimer (see below) (31–36).

Intrinsic Affinities of 181N-Terminal Domain - ssDNA Interactions

Binding of a single 181N-terminal domain dimer to 8-, 10-, 12-, 14-, 16-, 18-, 20-, and 24-mer can be analyzed using a single-site-binding isotherm described by

$$\Delta F=\Delta F_{max}\left[\frac{K_N P_F}{1+K_N P_F}\right] \quad (3)$$

where K_N is the macroscopic binding constant characterizing the affinity for a given ssDNA oligomer, containing N nucleotides, and ΔF_{max} is the maximum relative fluorescence increase. The solid lines in Figures 3a and 3c are nonlinear least-squares fits of the experimental titration curves using eq. 3, and a single set of binding and spectroscopic parameters for corresponding oligomers. The values of K_N for all studied ssDNA oligomers, which can accept only a single domain dimer, are included in Table 1.

Within experimental error, the value of K_N increases linearly with the length of the ssDNA oligomers (Table 1). This behavior indicates the presence of a statistical factor hidden in K_N and results from the fact that the number of nucleotides engaged in direct interactions with the ssDNA-binding site of the domain dimer, p, must be less than the length of the examined ssDNA oligomers (15–17,31–36). In other words, the 181N-terminal domain dimer experiences the presence of potential binding sites, with the direct intrinsic interactions characterized by the intrinsic binding constant, K_i. The determined macroscopic binding constant, K_N, is then defined as (15–17,31–36,49,50)

$$K_N = (N - p + 1) K_i \tag{4}$$

and

$$K_N = N K_i - (p - 1) K_i \tag{5}$$

Thus, K_N should be a linear function of N with the slope $\partial K_N/\partial N = K_i$. Moreover, for $K_N = 0$, the plot of K_N, as a function of the DNA length, will intercept the N axis at the value of $N = p - 1$.

The dependence of the macroscopic equilibrium constant, K_N, for the 181N-terminal domain dimer binding to the ssDNA oligomers, which can accept only a single dimer, as functions of the ssDNA oligomer length, is shown in Figure 6. The plot is strictly linear, as predicted by eqs. 4 and 5 (15–17,31–36,49,50). Extrapolation of the plot to the zero value of K_N intercepts the DNA length axis at $N = p - 1 = 4.2 \pm 1$. Thus the obtained data show that the 181N-terminal domain dimer engages in direct interactions with only $p = 5 \pm 1$ nucleotides of the nucleic acid (see Discussion). In the examined solution conditions, the slope of the plot in Figure 6 provides the intrinsic binding constant, $K_i = (1.6 \pm 0.3) \times 10^4$ M^{-1} (Table 1).

Intrinsic Affinities and Cooperativities of the 181N-Terminal Dimer Binding to the ssDNA Oligomers, Which Can Accept Two Dimer Molecules

For the ssDNA oligomers, 26-, 30-, and 33-mer, which can accept two 181N-terminal domain dimers the partition function, Z_N, must account for the potential overlap of the binding sites and the possible cooperative interactions between the bound dimer molecules (15–17,31–36,49,51–53). Such binding systems can be directly treated by the exact combinatorial theory for large ligand binding to a finite linear, homogeneous lattice (32–36,51–53). The partition function, Z_N, is defined as

$$Z_N = \sum_{k=0}^{g} \sum_{j=0}^{k-1} P_N(k, j) (K_i P_F)^k \omega^j \tag{6}$$

where g is the maximum number of ligand molecules which may bind to the finite nucleic acid lattice (for the nucleic acid lattice N residues long, $g = N/n$), ω is the cooperative interactions parameter, k is the number of ligand molecules bound, and j is the number of cooperative contacts between the k bound ligand molecules in a particular configuration on the lattice. The combinatorial factor $P_N(k, j)$ is the number of distinct ways that k ligands bind to a lattice, with j cooperative contacts, and is defined by

$$P_N(k,j)=\frac{[(N-nk+1)!(k-1)!]}{[(N-nk+j+1)!(k-j)!(k-j-1)!]} \quad (7)$$

The total average degree of binding, $\Sigma\Theta_i$, is then

$$\sum\Theta_i=\frac{\sum_{k=1}^{g}\sum_{j=0}^{k-1}kP_N(k,j)(K_i P_F)^k\omega^j}{\sum_{k=0}^{g}\sum_{j=0}^{k-1}P_N(k,j)(K_i P_F)^k\omega^j} \quad (8)$$

The value of the relative fluorescence increase, ΔF, at any titration point, is defined as

$$\Delta F=\Delta F_1\left\lfloor\frac{(N-n+1)K_i P_F}{Z_N}\right\rfloor+\Delta F_{max}\left[\frac{\sum_{j=0}^{k-1}P_N(k,j)(K_i P_F)^k\omega^j}{Z_N}\right] \quad (9)$$

where ΔF_1 and ΔF_{max} are the relative molar fluorescence increases accompanying the binding of one and two domain dimers. The values of the total site-size of the 181N-terminal domain - ssDNA complex, n = 13, is known (see above). The value of ΔF_1 can be estimated for each particular ssDNA oligomer as $\Delta F_1 = \partial\Delta F/\partial\,\Sigma\Theta_i$, from the initial part of the plot of ΔF as a function of $\Sigma\Theta_i$, as shown in Figure 4b for the 26-mer. The value of ΔF_{max} is the maximum observed relative fluorescence increase and can be estimated from the parental fluorescence titration curves, as shown in Figure 4a. Thus, two independent parameters, K_i and ω, must be determined. The solid lines in Figure 4a are nonlinear least-squares fits of the titration curves using eqs. 6 – 9. The obtained spectroscopic and binding parameters for all examined ssDNA oligomers, which can accommodate two domain dimers, are included in Table 1.

The values of the intrinsic binding constants for the 26-, 30-, and 33-mer are similar to each other and to the values of K_i, obtained for the oligomers accommodating only a single dimer molecule. Such similarity indicates that the same intrinsic binding process is observed, *i.e.*, the cooperative interactions do not affect the intrinsic affinity. The value of the cooperativity parameter, $\omega \approx 20 – 27$ is large, indicating the 181N-terminal domain dimer binds the ssDNA with significant positive cooperative interactions (15–17,31–36,49,51–53) (see Discussion). The value of ΔF_1, which characterizes the binding of the first dimer, is lower than those observed for most of the ssDNA oligomers, which accept only a single dimer and it decreases with the length of the oligomer (Table 1) (see Discussion).

Number of 181N-Terminal Domain Monomers Engaged in Interactions with the ssDNA. Photo-Cross-Linking Experiments

Next, we addressed the involvement of the monomers of the 181N-terminal domain dimer in interactions with the single-stranded nucleic acid using the UV irradiation method (19,46,48). UV irradiation produces covalent linkage between nucleic acid bases and amino acid residues, resulting in “zero-length” cross-linking with minimal perturbation to the

protein - nucleic acid complex (46). Among the nucleic acid bases, thymine is the most reactive in the photo-cross-linking reactions. Thus, parallel to the thermodynamic studies, we performed photo-cross-linking studies of the 181N-terminal domain complex with the radioactive [^{32}P]-dT_{20} (Materials & Methods). Only a single 181N-terminal domain dimer can associate with the ssDNA 20-mer (Table 1).

Figure 7a shows the SDS polyacrylamide gel of the 181N-terminal domain alone (lane 6) and the 181N-terminal domain - 5′ [^{32}P]-dT_{20} complex, after irradiation, at different protein concentrations, stained with Coomassie Brilliant Blue (Materials & Methods). In the case of the protein - nucleic acid complex, at the highest protein concentration applied, the nucleic acid is completely saturated with the protein (data not shown). A single protein band at ~21,000 indicates the location of the 181N-terminal domain monomer. Figure 7b shows the autoradiogram of the same SDS polyacrylamide gel of the 181N-terminal domain - 5′ [^{32}P]-dT_{20} complex. A single predominant radioactive band appears on the gel, at the molecular weight of ~26,000, corresponding to the 181N-terminal monomer - 20-mer complex. This band is undetectable on the Coomassie Brilliant Blue stained gel because of the very low efficiency of the photo-cross-linking reaction. The simplest explanation is that only one monomer of the 181N-terminal domain dimer principally engages the ssDNA in interactions in the complex. Nevertheless, a very slight radioactive band at the molecular weight of ~46,000, corresponding to the 181N- domain dimer, indicates that the DNA-binding subsite of the other monomer may engage the DNA, although at much lower efficiency (see Discussion) (19,46,48).

Base Specificity of 181N-Terminal Domain - ssDNA Interactions. Lattice Competition Titrations Using the MCT Method

Quantitative determination of affinities of the 181N-terminal domain for unmodified ssDNAs, differing by the type of base, has been performed, using the macromolecular competition titration (MCT) method (31,32,34,36). The approach is based on the same thermodynamic arguments as applied to quantitative titrations (Materials & Methods). In the presence of the competing unmodified ssDNA, the protein binds to two different nucleic acids that are present in the solution, while the observed signal originates only from the fluorescent “reference” nucleic acid. In this work we use, as a reference lattice, the 20-mer, $d\varepsilon A(p\varepsilon A)_{19}$, and the base specificity of the 181N-terminal domain has been examined using different 20-mers, $dN(pN)_{19}$. At a given titration point, “i”, the total concentration of the bound protein, P_b, is defined as (31,32,34,36)

$$P_b=(\sum\Theta_i)_R M_{TR}+(\sum\Theta_i)_S M_{TS} \quad (10)$$

were $(\Sigma\Theta_i)_R$ and $(\Sigma\Theta_i)_S$ are the total average degree of binding of the domain on the reference $d\varepsilon A(p\varepsilon A)_{19}$ and the examined oligomer, $dN(pN)_{19}$, respectively, M_{TR} and M_{TS} are the total concentrations of the reference and the unmodified 20-mer, respectively. Using the corresponding macroscopic binding constant, K_{NR} and K_{NS}, the above expression is defined as

$$P_b=\left(\frac{K_{NR}P_F}{1+K_{NR}P_F}\right)M_{TR}+\left(\frac{K_{NS}P_F}{1+K_{NS}P_F}\right)M_{TS} \quad (11)$$

The concentration of the free protein, P_F, is then

$$P_F = P_T - P_b \quad (12)$$

where P_T is the known total concentration of the 181N-terminal domain dimer. The observed relative fluorescence increase, ΔF, is then defined by eq. 5 (31,32,34,36).

Fluorescence titrations of dεA(pεA)$_{19}$ with the 181N-terminal domain in buffer C (pH 7.0, 10°C) in the presence of two different dA(pA)$_{19}$ concentrations, are shown in Figure 8a. For comparison, the titration curve of dεA(pεA)$_{19}$ in the absence of the competing oligomer is also included. The titration curve shifts, with increasing dA(pA)$_{19}$ concentration, indicating a significant competition between dεA(pεA)$_{19}$ and the unmodified 20-mer for the domain. Because $K_{NR} = 2.5 \times 10^5$ M^{-1} and $\Delta F_{max} = 1.15$ are known from independent titration experiments (Table 1), the solid lines in Figure 8a are nonlinear least-squares fits of the experimental titration curves, with a single fitting parameter, K_{NS}, using eqs. 10 – 12. The binding constants for all examined 20-mers, differing by the type of base, are included in Table 2. The obtained value of K_{NS} are similar for dA(pA)$_{19}$ and dT(pT)$_{19}$, respectively. Nevertheless, the domain shows modest preference for dC(pC)$_{19}$, with the intrinsic binding constant being higher by a factor of ~3 than the analogous parameter determined for the dA(pA)$_{19}$ and dT(pT)$_{19}$ (see Discussion).

DNA Conformation and 3′-End Specificities of 181N-Terminal Domain - ssDNA Interactions

The specific binding to the 3′-OH end group of deoxyribose by the PriA N-terminal domain, during the damaged DNA site recognition, has been invoked as the major feature, which allows the helicase to position itself on the nucleic substrate (14,18). Therefore, the effect of the presence of the phosphate group at the 3′-OH group, which blocks the access to the 3′-OH group of the terminal deoxyribose, on the 181N-terminal domain association with the ssDNA 20-mer, dC(pC)$_{18}$pCp, has been addressed using the MCT method (31,32,34,36) (see above). The homo-cytidine oligomer has been selected because of its highest affinity for the domain (Table 2). Fluorescence titrations of dεA(pεA)$_{19}$ with the 181N-terminal domain, in the absence of presence of two different concentrations of dC(pC)$_{18}$pCp, are shown in Figure 8b. As observed for dA(pA)$_{19}$ (Figure 8a), the titration curves significantly shift in the presence of dC(pC)$_{18}$pCp, indicating efficient competition for the domain by the oligomer. The solid lines in Figure 8b are nonlinear least-squares fits of the experimental titration curves, with a single fitting parameter, K_{NS}, using eqs. 10 – 12. It is clear that the obtained value of $K_{NS} = (1.6 \pm 0.3) \times 10^6$ M^{-1} is only by a factor of ~3 lower than determined for the analogous dC(pC)$_{19}$ (Table 2). Thus, the presence of the phosphate group, which blocks access to the 3′-OH terminal group of the ssDNA oligomer, has a rather modest effect on the 181N-terminal domain association (see Discussion). Finally, fluorescence titrations of dεA(pεA)$_{19}$ with the 181N-terminal domain, in the absence or presence of two different concentrations of the dsDNA 10-mer (Materials & Methods), are shown in Figure 8c. The solid lines in Figure 8c are nonlinear least-squares fits of the experimental titration curves with a single fitting parameter, K_{NS}, using eqs. 10 – 12. The obtained value of $K_{NS} = (3.0 \pm 1.0) \times 10^7$ M^{-1} is higher by a factor of ~6 than K_{NS} obtained for dC(pC)$_{19}$, and more than an order of magnitude higher than the macroscopic affinity of dA(pA)$_{19}$, and dT(pT)$_{19}$ (Table 2) (see Discussion).

Salt Effect on the 181N-Terminal Domain - ssDNA Interactions

Fluorescence titrations of dεA(pεA)$_{17}$ with the 181N-terminal domain dimer, in buffer C (pH 7.0, 10°C) containing different NaCl concentrations, are shown in Figure 9a. The dimer preserves its oligomeric structure in the examined salt concentration range (data not shown). Increasing the salt concentration in solution clearly decreases the macroscopic affinity of the

domain for the nucleic acid, as the titration curves shift toward higher protein concentrations range. Also, there is a decline of the maximum fluorescence increase at saturation, ΔF_{max}, from ~1.9 at 20 mM to ~1.2 at 88.6 mM NaCl, indicating the changing structure of the nucleic acid in the complex. The solid lines in Figures 9a are nonlinear least-squares fits to a single-site binding model with two fitting parameters, K_N, and the maximum relative fluorescence increase, ΔF_{max} (eq. 3). Figure 9b shows the dependence of the logarithm of K_N upon the logarithm of the NaCl concentration (log-log plots) (54,55). Within experimental accuracy, the plot is linear in the examined salt concentration range and characterized by the slopes $\partial \log K_N / \partial \log[NaCl] = -1.2 \pm 0.3$. The value of the slope indicates that there is a net release of ~1 ion upon the complex formation (see Discussion) (54,55).

Binding of Nucleotide Cofactors to the 181N-Terminal Domain of the PriA Helicase

As mentioned above, the intact PriA helicase has two nucleotide binding sites dramatically differing in their affinities, *i.e.*, the strong and weak binding sites (19–23). However, the location of these sites, with respect to the domain structure of the protein, is unknown. We have found that similar to the intact PriA protein, the ADP analog, TNP-ADP, binds to the 181N-terminal domain. The use of TNP-analog was dictated by the fact that it has a high affinity for the PriA nucleotide-binding sites, which facilitated the binding analysis (19–23). Moreover, the association is accompanied by strong quenching of the protein fluorescence, providing the required signal to monitor the association process (20,21,23). Fluorescence titrations of the 181N-terminal domain with TNP-ADP, at three different protein concentrations, in buffer C (pH 7.0, 10°C), are shown in Figure 10a. The maximum quenching of the protein fluorescence at saturation is 1.0 ± 0.05 (see Discussion). The selected protein concentrations provide separation of the titration curves up to a quenching value of ~0.65.

Quantitative analysis of the titration data has been performed using the quantitative method, analogous to the approach applied in the nucleic acid binding studies and outlined in Materials & Methods (15–17,31–36,49,51–53). The dependence of the observed relative fluorescence quenching, ΔF, upon the total average degree of binding, $\Sigma\Theta_i$, of TNP-ADP on the 181N-terminal domain dimer is shown in Figure 10b. The separation of the titration curves allows us to obtain the values of $\Sigma\Theta_i$ up to ~1.5 TNP-ADP molecules per dimer. The plot is, within experimental accuracy, linear. Extrapolation to the maximum value of the quenching provides the stoichiometry of the complex as 2.2 ± 0.2. Therefore, the data show that the 181N-terminal domain dimer binds two molecules of TNP-ADP, indicating that each monomer binds a single nucleotide cofactor molecule.

Statistical Thermodynamic Model for Nucleotide Cofactor Binding to the 181N-Terminal Domain Dimer

Because of the 181N-terminal domain dimer is built of two identical monomers, the two nucleotide-binding sites must be structurally identical, although they may be energetically different (see Discussion). Therefore, the simplest statistical thermodynamic model, *i.e.*, the model containing the fewest number of parameters, that can account for the observed binding process includes two nucleotide-binding sites, characterized by two different intrinsic affinities described by intrinsic binding constant, K_{C1} and K_{C2}, respectively, and possible cooperative interactions between the sites, accounted for by the cooperative interaction parameter, σ. The partition function, Z, of the system is then defined as

$$Z = 1 + (K_{C1} + K_{C2}) L_F + K_{C1} K_{C2} \sigma L_F^2 \quad (13)$$

where L_F is the free nucleotide cofactor concentration. The total average degree of binding, $\Sigma\Theta_i$, is defined as

$$\sum\Theta_i=\frac{(K_{C1}+K_{C2})L_F+2K_{C1}K_{C2}\,\sigma L_F^2}{Z} \quad (14)$$

The linear character of the plot in Figure 10b indicates that binding of the first and second cofactor molecules is characterized by the same relative partial quenching of the protein tryptophans. Therefore, experimentally observed fluorescence quenching, ΔF, expressed in terms of the binding parameters, K_C and σ, is then

$$\Delta F=\Delta F_{max}\left(\frac{(K_{C1}+K_{C2})L_F+K_{C1}K_{C2}\,\sigma L_F^2}{Z}\right) \quad (15)$$

There are three unknown parameters, K_{C1}, K_{C2}, and σ in eqs. 13 – 15. The solid lines in Figure 10a are the nonlinear least-squares fits of the titration curves using eqs. 13 – 15, with a single set of spectroscopic and binding parameters. The fit provides an excellent description of the binding process. The obtained intrinsic binding constants and cooperativity parameters are: $K_{C1} = K_{C2} = (4.1 \pm 0.6) \times 10^4\ M^{-1}$ and $\sigma = 1 \pm 0.2$, respectively. The same values of both intrinsic binding constants indicate that the nucleotide cofactor sites are not only structurally but also energetically identical (see Discussion). Moreover, the value of $\sigma \approx 1$ indicates that binding of the cofactor to two nucleotide-binding sites of the 181N-terminal dimer is not characterized by any cooperative interactions (see Discussion).

In the same solution conditions as applied in this work, TNP-ADP binds to the strong and weak nucleotide-binding sites of the intact PriA helicase with the intrinsic binding constants: $K_S = (1.5 \pm 0.5) \times 10^6\ M^{-1}$, $K_W = (1.9 \pm 0.6) \times 10^4\ M^{-1}$, respectively, and the cooperativity parameter, $\sigma = 1 \pm 0.3$ (20,21,23). Thus, the intrinsic binding constants of the two sites of the intact enzyme differ by ~2 orders of magnitude. Such a dramatic difference between the affinities of the two nucleotide-binding sites of the intact PriA protein facilitates the assignment of the nucleotide-binding site of the 181N-terminal domain. Figure 10c shows the dependence of $\Sigma\Theta_i$ of the TNP-ADP on the intact PriA helicase and the isolated 181N-terminal domain dimer as function of the free cofactor concentration. The plots have been generated using the binding parameters for the intact enzyme and the 181N-terminal domain dimer (see above). The isotherm for the 181N-terminal domain is strongly shifted toward the higher nucleotide concentration range. In other words, it reflects the cofactor association with the weak nucleotide-binding site of the intact PriA protein, as expressed by the value of $K_C \approx 4.1 \times 10^4\ M^{-1}$, being very close to the intrinsic binding constant, $K_S \approx 1.9 \times 10^4\ M^{-1}$, of the weak nucleotide-binding site (see above). Thus, the obtained data indicate that the nucleotide-binding site located on the N-terminal domain corresponds to the weak nucleotide-binding site of the intact PriA helicase (see Discussion).

Association of the 181N-Terminal Domain Dimer With the ssDNA in the Presence of ADP or ATPγS

Characteristic feature of the nucleotide effect on the intact PriA helicase association with the ssDNA is that saturation of the weak nucleotide-binding site with ADP but not ATP analog, ATPγS, dramatically increases the enzyme affinity for the nucleic acid (23). On the other hand, saturation of only the strong nucleotide-binding site with ADP or ATPγS has no effect

on the enzyme ssDNA-affinity. Fluorescence titrations of the ssDNA 18-mer, dεA(pεA)$_{17}$, with the 181N-termninal domain in buffer C (pH 7.0, 10°C), in the absence and presence of two different concentrations of ADP, are shown in Figure 11a. The solid lines in Figure 11a are nonlinear least-squares fits of the titration curves, using the single-site binding isotherm (eq. 3). The presence of [ADP] = 1×10^{-5} M, which would fill the strong nucleotide-binding site of the intact enzyme, leaves the 181N-terminal domain affinity for the ssDNA practically unaffected with $K_N = (1.9 \pm 0.4) \times 10^5$ M^{-1}, as compared to $K_N = (2.2 \pm 0.4) \times 10^5$ M^{-1}, determined in the absence of the cofactor (see above). However, at [ADP] = 3×10^{-3} M, which saturates the 181N-terminal nucleotide binding site, as well as the weak nucleotide-binding site of the intact PriA, the affinity of the domain for the nucleic acid is increased by a factor of ~5 with a concomitant increase of ΔF_{max} (see Discussion) (20,21,23).

Analogous fluorescence titrations of the ssDNA 18-mer, dεA(pεA)$_{17}$, with the 181N-terminal domain in the absence and presence of ATPγS, at two different concentrations of the nucleotide cofactor, are shown in Figure 11b. The effect of the nucleoside tri-phosphate is very different from the effect of ADP (Figure 11a). At a low concentration of ATPγS (1×10^{-4} M), which would saturate the strong nucleotide-binding site of the intact PriA protein, the ssDNA affinity of the domain detectably decreases to $K_N = (1.4 \pm 0.3) \times 10^5$ M^{-1} with no effect on the observed ΔF_{max}. Similarly, at [ATPγS] = 3×10^{-3} M, which saturates both the strong and weak nucleotide-binding sites of the intact enzyme and the nucleotide-binding sites of the 181N-terminal domain, the value of K_N is hardly affected by the cofactor ($K_N = (1.8 \pm 0.4) \times 10^5$ M^{-1}), as compared to the affinity obtained in the absence of ATPγS, although the value of the observed ΔF_{max} is slightly decreased (see Discussion) (23).

DISCUSSION

Formation of the Dimer By the Isolated N-Terminal Domain May Indicate That the Cooperative Interactions of the Intact PriA Protein With the dsDNA Involve the N-Terminal Domain of the Protein

The intact PriA helicase exists in solution as a monomer (15–17,21–23). Yet, the isolated 181N-terminal domain of the protein forms a stable dimer (Figure 2). Similarly, a dimeric form of the truncated 105N-terminal subdomain has been seen in the crystal and in solution (18). The crystal structure of the 105N-terminal subdomain dimer (Figure 1b) indicates that the monomers interact through the N-terminal fragments (intervening dimer). Similar interactions, if present in solution, may occur in the case of the complete 181N-terminal domain, although it has an extra subdomain, comprising an additional 76 amino acid residues, at its C-terminus. Nevertheless, these data suggest that the 181N-terminal domain monomers may directly interact through their N-terminal subdomains.

Recall, the PriA helicase binds the ssDNA in a noncooperative fashion (15–17). However, binding of the enzyme to the dsDNA is characterized by positive cooperativity (19). We have previously discussed the role of the positive cooperativity in the enzyme binding to the dsDNA as playing a role in the gapped-DNA recognition by the PriA protein (22). In the complex with the dsDNA, the PriA helicase assumes a very different orientation, as compared to the complex with the ssDNA and occludes only ~5 base pairs of the nucleic acid (19,23). In this orientation, the helicase engages in the complex only its strong DNA-binding subsite located on the helicase domain, which leaves the N-terminal domain free to engage in cooperative interactions (19,23). The observed formation of the dimer by the 181N-terminal domain may reflect the propensity of the domain to engage in cooperative interactions when it is a part of the intact enzyme molecule. It should be pointed out that binding of the 181N-terminal domain dimer to the ssDNA oligomers, which can accept

more than one dimer molecule, is also accompanied by significant positive cooperative interactions (Table 1). However, these interactions are too weak for detectable formation of the domain oligomers higher than the dimer.

The 181N-Terminal Domain Dimer Has Only One Effective ssDNA-Binding Site

The 181N-terminal domain dimer is built of two identical monomers and it possesses two structurally identical and potential DNA-binding sites, each located on a different monomer. Thus, crystallographic analyses of the 105N-terminal subdomain dimer suggest that the dimer has two DNA-binding sites, though not necessarily energetically equivalent ones (see below) (18). On the other hand, thermodynamic and photo-cross-linking data show that, in solution, only a single monomer of the 181N-terminal domain predominantly engages the ssDNA (Figures 3 and 7, Table 1). Notice, only a single domain dimer binds to the 20- or 24-mer, although the length of these oligomers is large enough to fully access to the DNA-binding site on the second monomer (Figure 6, Table 1). In fact, the photo-cross-linking data indicate that the second monomer of the 181N-terminal domain may very weakly engage the nucleic acid (Figure 7b).

Nevertheless, the local concentration of these longer oligomers in the complex with the domain dimer is very high. Thus, the affinity of the second binding site must be very low, otherwise it would be easily accessed by the long oligomers and manifested in a large change in the total site-size of the complex, and the intrinsic affinity. However, this is not experimentally observed (Figures 5 and 6). The total site-size of the 181N-terminal dimer complexes with the longer oligomers is 13 ± 1 nucleotides and the intrinsic affinity is, within experimental accuracy, the same as the corresponding affinity of the shorter oligomers (Table 1). The lack of any significant DNA-binding activity of the second monomer of the 181N-terminal domain dimer with ssDNA oligomer, which encompass the site-size of ~5 nucleotides of the DNA-binding subsite, most probably results from a steric hindrance induced by the active monomer and its 76 amino acids long C-terminal subdomain (Figure 7c).

The Small Number of Nucleotides Engaged in Direct Interactions with the ssDNA Indicates That the DNA-Binding Subsites of the PriA Helicase Are Spatially Separated in the Intact Enzyme

The binding site of the 181N-terminal domain engages in direct interactions only ~5 nucleotides of the ssDNA (Figure 6). Such a small site-size provides further indication that only one monomer of the dimer interacts with the nucleic acid (see above). Notice, the maximum relative fluorescence increase of the etheno-adenosine ssDNA oligomers, ΔF_{max}, induced upon the domain binding, gradually decreases with the length of the oligomer (Table 1). This behavior is expected, as the number of the nucleotides in the nucleic acid increases, while the number of the nucleotides directly engaged in interactions with the protein (~5) remains unchanged. Recall, the total site-size of the DNA-binding site of the intact PriA helicase is ~20 nucleotides, while the site-size of the strong DNA-binding subsite on the helicase domain is only ~6 nucleotides (15–17,19–23). Thus, when both subsites interact with the nucleic acid, *e.g.*, when both nucleotide-binding sites are saturated with ADP, the intact enzyme engages in direct interactions only ~10 – 11 nucleotides of the DNA out of a total of ~20 nucleotides (15–17,19–23). These data suggest that the strong DNA-binding subsite on the helicase domain and the subsite on the N-terminal domain are spatially separated in the intact enzyme molecule by a distance corresponding to ~3 – 5 nucleotides of the ssDNA, *i.e.*, they do not form a structurally continuous entity.

The DNA-Binding Subsite of the Isolated 181N-Terminal Domain Is In an Open Conformation Indicating the Presence of Domain - Domain Interactions in the Intact Enzyme

In the case of the intact PriA helicase the DNA-binding subsite of the N-terminal domain becomes involved in interactions with the ssDNA, only in the presence of ADP concentrations, which is high enough to saturate the weak nucleotide-binding site (21). As we previously proposed, the subsite on the N-terminal domain must be in a “closed” conformation in the intact enzyme and transforms to the “open” conformation in the presence of high [ADP] (21). On the other hand, the isolated domain is able to efficiently bind the nucleic acid in the absence of the cofactor, although with lower affinity (Table 1). If the DNA-binding subsite in the intact enzyme was in open conformation, the intrinsic ssDNA-affinity of the isolated 181N-terminal domain subsite, even in the absence of ADP, would be too high to prevent the subsite to engage in interactions with the ssDNA in the intact enzyme (Tables 1 and 2). The fact that the isolated domain associates with the nucleic acid, even in the absence of ADP, indicates that its DNA-binding subsite is in the “open” conformation. Furthermore, these data also indicate that the interactions of the 181N-terminal domain with the nucleic acid, *i.e.*, the transition from closed to open conformations, are affected by the inter-domain interactions with the helicase domain in the intact PriA helicase.

181N-Terminal Domain DNA-Binding Subsite Has Only a Slight Preference For the 3′ End of the Nucleic Acid

The specific binding of the N-terminal domain subsite to the deoxyribose OH group at the 3′ end of the nucleic acid has been invoked as an important factor in the recognition of the damaged replication fork by the PriA helicase, even in the absence of the nucleotide cofactors (see below) (14,18). However, quantitative thermodynamic and kinetic analyses of the enzyme binding to the ssDNA oligomer, reported in our previous works, did not indicate the presence of any significant and/or specific affinity of the intact enzyme for the 3′ end of the nucleic acid (15–17,21–23). Moreover, the enzyme binds the gapped DNA substrates using its strong DNA-binding subsite on the helicase domain, not the weak subsite of the 181N-terminal domain (22). In the case of the isolated 181N-terminal domain, blocking the 3′end OH group of the ssDNA by the phosphate group only slightly decreases by a factor of ~3 the intrinsic affinity (Table 2). Therefore, at present time, it is not clear what role, if any, a modest affinity difference by a factor of ~3 plays a role in specific enzyme binding to the damaged DNA substrate, particularly in the presence of large local concentrations of different DNA conformations (see below).

The 181N-Terminal Domain Has a Significant Affinity For the dsDNA

In the context of the previous section, the 181N-terminal domain has a surprisingly high affinity for the dsDNA (Figure 8c, Table 2). If the site-size of the domain is the same as determined for the ssDNA (~5 nucleotides or correspondingly ~5 base pairs), then the intrinsic affinity is by a factor of ~20 – 50 higher than that determined for the ssDNA oligomers, including, $dC(pC)_{18}pCp$ and $dC(pC)_{18}$ (Table 2). It is possible that the dsDNA affinity, not the 3′end-OH group affinity, plays a role in the recognition of the damaged DNA by the N-terminal domain in the stalled replication fork. Further quantitative studies are necessary to assess the role of the 3′end-OH group and the dsDNA affinity of the N-terminal domain in specific recognition of the damaged replication fork by the PriA helicase.

The DNA-Binding Subsite of the 181N-Terminal Domain Lacks Significant Base Specificity in Interactions With the ssDNA

The strong DNA-binding subsite of the intact PriA helicase shows a significant preference for the pyrimidine homo-oligomers, with the intrinsic binding constant being ~1 order of magnitude higher for the $dT(pT)_{19}$ and $dC(pC)_{19}$ than that observed for $dA(pA)_{19}$ or $d\varepsilon A(p\varepsilon A)_{19}$ (16). On the other hand, the DNA-binding subsite located of the N-terminal domain has only a small preference for $dC(pC)_{19}$, as compared to other unmodified oligomers (Table 2). Interestingly, unlike the strong subsite on the helicase domain, the 181N-terminal domain subsite has a pronounced lower affinity for the etheno-modified oligomers than for all other examined nucleic acids (Table 2). Moreover, in similar solution conditions, the 181N-terminal domain subsite has the intrinsic ssDNA-affinity lower by a factor of ~ 6 – 7 than the intrinsic DNA affinity of the strong subsite (15,16). The data indicates that two DNA-binding subsites of the PriA helicase differ significantly in their nature of interactions with the ssDNA. This difference is further indicated by the salt effect on the corresponding interactions. While the DNA binding to the strong subsite is accompanied by the net release of ~3 – 4 ions, binding to the 181N-terminal domain subsite induces the net release of only ~1 ion (Figure 9b) (16).

The Weak Nucleotide-Binding Site of the Intact PriA Helicase Is Located on the 181N-Terminal Domain

As mentioned above, the difference between the PriA protein and other well-studied monomeric helicases is the fact that the protein possesses two nucleotide-binding sites, strong and weak binding sites (20,21,23). First, the discovery that the isolated 181N-terminal domain possesses a nucleotide-binding site firmly places one of these sites on the N-terminal domain of the intact protein. Moreover, the low intrinsic affinity, very similar to the affinity of the weak nucleotide-binding site of the intact enzyme, provides the first indication that the site located on the N-terminal domain corresponds to the weak nucleotide-binding site of the intact PriA helicase (see above). By the same token, the strong nucleotide-binding site must be located on the helicase domain of the enzyme.

Another indication that the nucleotide-binding site on the N-terminal domain corresponds to the weak site of the intact enzyme comes from the effect of the cofactors on the nucleic acid binding. Only when the nucleotide-binding site is saturated with ADP, the ssDNA affinity of the DNA-binding subsite of the domain strongly increases (Figure 11a), while saturation of the site with the ATP nonhydrolyzable analog, ATPγS, leads to a slightly diminished affinity for the nucleic acid (Figure 11b). This is exactly the behavior, which is observed in the case of the weak nucleotide-binding site of the PriA helicase (22,23). The weak nucleotide-binding site acts as an allosteric site, which controls the engagement of the N-terminal domain into the interactions with the DNA (22,23). Moreover, the data indicate that the observed allosteric effect of the weak nucleotide-binding site is localized on the N-terminal domain.

The presence of two nucleotide-binding sites on the domain dimer indicates that each monomer of the dimer binds a single cofactor molecule. Thus, unlike the ssDNA-binding subsites (see above), both nucleotide-binding sites are accessible on the domain dimer and the binding process is independent. Notice, binding of TNP-ADP induces ~100% quenching of the 181N-terminal domain tryptophan fluorescence (Figure 10a). Moreover, the quenching is the same for each binding site. Although TNP moiety is an excellent fluorescence energy transfer acceptor from tryptophans, the cofactor cannot be at close proximity to all 5 tryptophan residues of each monomer of the dimer. Such large quenching must result from a significant conformational transition of the domain induced by the cofactor binding, leading to additional quenching of the protein tryptophans.

The ADP Effect on the 181N-Terminal Domain DNA-Binding Subsite Indicates That in the Intact Enzyme ADP Not Only Opens the Subsite But Also Increases Its Intrinsic ssDNA Affinity

The finding that saturation of the nucleotide-binding site of the 181N-terminal domain with ADP increases the affinity of the DNA-binding subsite corroborates the conclusion that the nucleotide cofactor induces a major conformational transition of the domain (see above). Nevertheless, the process is different from the analogous effect in the case of the intact enzyme, where the DNA-binding subsite is in a closed conformation in the absence of high [ADP] and does not manifest any DNA-binding activity (15–17,22,23). In the isolated domain, the DNA-binding subsite is already open and has a substantial DNA affinity in the absence of ADP. These data indicate that the allosteric effect of ADP in the weak nucleotide-binding site of the intact enzyme, on the DNA-binding subsite of the N-terminal domain, not only opens the subsite and enables the nucleic acid to enter it, but also affects the intrinsic DNA affinity of the subsite.

Comparison with Other Works

The crystallographic data on the truncated 105N-terminal subdomain dimer indicate that the DNA-binding subsite of the complete 181N-terminal domain is located on the 105N-terminal subdomain, *i.e*., further away from the helicase domain and corroborating our conclusion that the DNA subsites of the intact enzyme are spatially separated (18). However, the data also indicate that the 105N-terminal subdomain dimer can bind two nucleic acid molecules, while thermodynamic data and photo-cross-linking discussed in this work show the presence of only one effective DNA-binding subsite. However, the examined crystallographic complexes of the 105N-terminal subdomain involved very short di- and tri-nucleotides, which may not reflect the interactions with the longer nucleic acids (18). The truncated subdomain may have a different conformation and the resulting different access of the DNA to the binding sites, as compared to the 181N-terminal domain. It should be pointed out that the conserve motif (W83, Y87, Y88), previously proposed to be involved in the DNA binding to the N-terminal domain, is not present in the vicinity of the determined DNA-binding site in the crystal structure (14,18).

A puzzling previous result is that the 105N-terminal subdomain dimer showed the highest macroscopic affinity for the short oligomers (~4 nucleotides) and its macroscopic DNA-affinity decreases with the length of the nucleic acid (18). As we discussed above, unlike the intrinsic affinity, the macroscopic affinity is affected by the length of the ssDNA, because of the presence of the statistical factor, which increases with the length of the nucleic acid and positively contributes to the obtained free energy of binding (eqs. 6 and 7). In other words, macroscopic affinity is not a parameter, which can provide a clear estimate of the preferential association. Moreover, a factor of ~6 lower affinity of the 105N subdomain, for oligomers with the 3′end-OH group blocked by the phosphate group was also reported, as compared to the factor of ~3 found in this work (18). We cannot explain all the differences. Nevertheless, in these previous studies, neither the intrinsic affinity nor the stoichiometries have been determined (18). The reported titration curves do not have plateaus, which prevents any quantitative analyses. The macroscopic affinity estimates were based on qualitative comparisons of apparent translational diffusion coefficients of the complexes, with a large inherent error of the applied method, and with the values of the diffusion parameter being, within experimental accuracy, the same for the ssDNAs containing from 2 to 7 nucleotides (18). Moreover, the reported lower value of the diffusion parameter for the wild-type protein at higher protein concentrations in different sets of data is inconsistent, as a higher value of the parameter at a higher protein concentration should be observed (18).

Further Functional Implications

The large differences between the two DNA-binding subsites of the *E. coli* PriA helicase in their affinities, base specificities, and nucleotide effects must reflect the differences in functional roles of both sites in the PriA activities (19,21,22). A significant preference of the strong DNA-binding subsite on the helicase domain for homo-pyrimidine oligomers coincides with the overwhelming preference of the PriB protein for homo-thymine ssDNAs (31). The PriA - PriB complex is one of two major pathways for restarting the chromosomal DNA replication in *E. coli* at the damaged DNA site (9,10–13). The preference for pyrimidine stretches of both proteins strongly suggests that the sequence of the nucleic acid around the damaged DNA site plays an important role in the damage recognition process and in the selection of the pathway to restart the replication fork, with the strong DNA-binding subsite of the PriA helicase involved in the reactions. Moreover, stopped-flow kinetic data showed that the strong subsite on the PriA helicase domain is the area, which makes the first contact with the nucleic acid in the enzyme association reaction (17). Furthermore, the strong subsite plays a major role in the recognition of the ss-ds junctions in the gapped DNA substrates, specifically matching the size of the ssDNA gap with 5 nucleotides (22).

In all these activities of the intact enzyme, the subsite on the N-terminal domain is absent, or its role is secondary (22). Its decisive presence appears only when the weak nucleotide-binding site of the PriA protein is saturated with ADP (21). The ssDNA affinity of the N-terminal domain subsite is dramatically controlled by the nucleotide cofactors, while the control of the DNA affinity of the strong subsite is, if any, very modest (21,22). Moreover, the 181N-terminal domain DNA-binding subsite has very low, if any, base specificity (Table 2). These differences point to the strong subsite as the major recognition site of the DNA structures and/or conformations, while the N-terminal subsite predominantly becomes involved during the mechanical translocation and the dsDNA unwinding by the PriA helicase, where the nucleotide control of the nucleic acid affinity is crucial and the base/sequence specificity is not necessary (56–58). In this endeavor, the subsite on the 181N-terminal domain would be the DNA-binding subsite of the PriA protein essential for the efficient energy transduction process. Our laboratory is currently examining these processes.

Acknowledgments

We wish to thank Mrs. Gloria Drennan Bellard for reading the manuscript.

Abbreviations

ssDNA	single-stranded DNA
dsDNA	double-stranded DNA
dNTP	deoxy-nucleoside 5′ triphosphate
εA	etheno-adenosine
DTT	dithiothreitol
bps	base-pairs
ADP	adenosine-5′-diphosphate
TNP-ADP	2′(3′)-O-(2,4,6-trinitrophenyl)adenosine 5′-diphosphate
DEAE cellulose	Diethylaminoethyl cellulose

References

1. Kornberg, A.; Baker, TA. DNA Replication. Freeman; San Francisco: 1992. p. 275-293.
2. Shlomai J, Kornberg A. An *Escherichia coli* Replication Protein That Recognizes a Unique Sequence Within a Hairpin Region in ΩX174 DNA. Proc Natl Acad Sci USA. 1980; 77:799–803. [PubMed: 6444725]
3. Wickner S, Hurwitz J. Association of phiX174 DNA-dependent ATPase Activity With an *Escherichia coli* Protein, Replication factor Y, Required For *in vitro* Synthesis of phiX174 DNA. Proc Natl Acad Sci U S A. 1975; 72:3342–3346. [PubMed: 127175]
4. Marians KJ. PriA: at the Crossroads of DNA Replication and Recombination. Prog Nucleic Acid Res, Mol Biol. 1999; 63:39–67. [PubMed: 10506828]
5. Shlomai J, Kornberg A. Prepriming DNA Replication Enzyme of *Escherichia coli* I Purification of Protein n': a Sequence-Specific, DNA-Dependent ATPase. J Biol Chem. 1980; 255:6789–6793. [PubMed: 6104665]
6. Jones JM, Nakai H. Duplex Opening by Primosome Protein PriA for Replisome Assembly on a Recombination Intermediate. J Mol Biol. 1999; 289:503–516. [PubMed: 10356325]
7. Greenbaum JH, Marians KJ. Mutational Analysis of Primosome Assembly Site. Evidence For Alternative Structures. J Biol Chem. 1985; 260:12266–12272. [PubMed: 2931433]
8. Ng JY, Marians KJ. The Ordered Assembly of the fX174 Primosome. II Preservation Primosome Composition From Assembly Through Replication. J Biol Chem. 1996; 271:15649–15655. [PubMed: 8663105]
9. Sangler SJ. Requirements For Replication Restart Proteins During Constitutive Stable DNA replication in *Escherichia coli* K-12. Genetics. 2005; 169:1799–1806. [PubMed: 15716497]
10. Allen GC, Kornberg A. Assembly of the Primosome of DNA Replication in *Escherichia coli*. J Biol Chem. 1993; 268:19204–19209. [PubMed: 8366072]
11. Arai K, Arai N, Shlomai J, Kornberg A. Replication of the Duplex DNA of Phage PhiX174 Reconstituted with Purified Enzymes. Proc Acad Sci USA. 1981; 77:3322–3326.
12. Heller RC, Marians KJ. Replication Fork Reactivation Downstream of the Blocked Nascent Leading Strand. Nature. 2006; 439:557–562. [PubMed: 16452972]
13. Heller RC, Marians KJ. Non-Replicative Helicases at the Replication Fork. DNA Repair. 2007; 6:945–952. [PubMed: 17382604]
14. Tanaka T, Mizukoshi T, Taniyama C, Kohda D, Arai K-I, Masai H. DNA-Binding of PriA Protein Requires Cooperation of the N-Terminal D-Loop/Arrested-Fork Binding and C-Terminal Helicase Domains. J Biol Chem. 2002; 277:38062–38071. [PubMed: 12151393]
15. Jezewska MJ, Rajendran S, Bujalowski W. *Escherichia coli* Replicative Helicase PriA Protein - Single-Stranded DNA Complex. Stoichiometries, Free Energy of Binding, and Cooperativities. J Biol Chem. 2000; 275:27865–27873. [PubMed: 10875934]
16. Jezewska MJ, Bujalowski W. Interactions of *Escherichia coli* Replicative Helicase PriA Protein with Single-Stranded DNA. Biochemistry. 2000; 39:10454–10467. [PubMed: 10956036]
17. Galletto R, Jezewska MJ, Bujalowski W. Multi-Step Sequential Mechanism of *E. coli* Helicase PriA Protein – ssDNA Interactions. Kinetics and Energetics of the Active ssDNA-Searching Site of the Enzyme. Biochemistry. 2004; 43:11002–11016. [PubMed: 15323559]
18. Sasaki K, Ose T, Okamoto N, Maenaka K, Tanaka T, Masai H, Saito M, Shirai T, Kohda D. Structural Basis of the 3′-end Recognition of a Leading Strand in Stalled Replication Fork by PriA. EMBO J. 2007; 26:2584–2593. [PubMed: 17464287]
19. Szymanski MR, Jezewska MJ, Bujalowski W. The *Escherichia coli* PriA Helicase - Double-Stranded DNA Complex. Location of the Strong DNA-Binding Subsite on the Helicase Domain of the Protein and the Affinity Control By the Two Nucleotide-Binding Sites of the Enzyme. J Mol Biol. 2010; 402:344–362. [PubMed: 20624397]
20. Lucius AL, Jezewska MJ, Bujalowski W. The *Escherichia coli* PriA Helicase Has Two Nucleotide-Binding Sites Differing in Their Affinities for Nucleotide Cofactors. 1 Intrinsic Affinities, Cooperativities, and Base Specificity of Nucleotide Cofactor Binding. Biochemistry. 2006; 45:7202–7216. [PubMed: 16752911]

21. Lucius AL, Jezewska MJ, Bujalowski W. Allosteric Interactions Between the Nucleotide-Binding Sites and the ssDNA-Binding Site in the PriA Helicase – ssDNA Complex, 3. Biochemistry. 2006; 45:7217–7236. [PubMed: 16752912]
22. Szymanski MR, Jezewska MJ, Bujalowski W. The *E. coli* PriA Helicase Specifically Recognizes Gapped DNA Substrates. Effect of the Two Nucleotide-Binding Sites of the Enzyme on the Recognition Process. J Biol Chem. 2010; 285:9683–9696. [PubMed: 20089865]
23. Lucius AL, Jezewska MJ, Bujalowski W. Biochemistry. 2006; 45:7217–7236. [PubMed: 16752912]
24. Edeldoch H. Spectroscopic Determination of Tryptophan and Tyrosine in Proteins. Biochemistry. 1967; 6:1948–1954. [PubMed: 6049437]
25. Gill SC, von Hippel PH. Calculation of Protein Extinction Coefficients From Amino Acid Sequence Data. Anal Biochem. 1989; 182:319–326. [PubMed: 2610349]
26. Jezewska MJ, Galletto R, Bujalowski W. Rat Pol β Binds Double-Stranded DNA Using Exclusively the 8-kDa Domain. Stoichiometries, Intrinsic Affinities, and Cooperativities. Biochemistry. 2003; 42:5955–5970. [PubMed: 12741854]
27. Jezewska MJ, Galletto R, Bujalowski W. Tertiary Conformation of the Template-Primer and Gapped DNA Substrates in Complexes With Rat Polymerase β. Fluorescence Energy Transfer Studies Using the Multiple Donor-Acceptor Approach. Biochemistry. 2003; 42:11864–11878. [PubMed: 14529299]
28. Ledneva RK, Razjivin AP, Kost AA, Bogdanov AA. Interaction of Tobacco Mosaic Virus Protein With Synthetic Polynucleotides Containing a Fluorescent Label: Optical Properties of poly(εA) and poly(εC) Copolymers and Energy Migration From the Tryptophan to $1,N^6$-Ethenoadenine or $3,N^4$-Ethenocytosine Residues in RNP. Nucleic Acids Res. 1978; 5:4225–4243. [PubMed: 724512]
29. Tolman GL, Barrio JR, Leonard NJ. Choroacetaldehyde-Modified Dinucleoside Phosphates. Dynamic Fluorescence Quenching and Quenching Due to Intramolecular Complexation. Biochemistry. 1974; 13:4869–4878. [PubMed: 4373039]
30. Baker BM, Vanderkooi J, Kallenbach NR. Base Stacking In a Fluorescent Dinucleoside Monophosphate: εApεA. Biopolymers. 1978; 17:1361–1372.
31. Szymanski MR, Jezewska MJ, Bujalowski W. Interactions of the *Escherichia coli* Primosomal PriB Protein with the Single-Stranded DNA. Stoichiometries, Intrinsic Affinities, Cooperativities, and Base Specificities. J Mol Biol. 2010; 398:8–25. [PubMed: 20156448]
32. Bujalowski W. Thermodynamic and Kinetic Methods of Analyses of Protein – Nucleic Acid Interactions. From Simpler to More Complex Systems. Chem Rev. 2006; 106:556–606. [PubMed: 16464018]
33. Lohman TM, Bujalowski W. Thermodynamic Methods for Model-Independent Determination of Equilibrium Binding Isotherms for Protein-DNA Interactions: Spectroscopic Approaches to Monitor Binding. Meth Enzym. 1991; 208:258–290. [PubMed: 1779838]
34. Jezewska MJ, Bujalowski W. A General Method of Analysis of Ligand Binding to Competing Macromolecules Using the Spectroscopic Signal Originating from a Reference Macromolecule. Application to *Escherichia coli* Replicative Helicase DnaB Protein-Nucleic Acid Interactions. Biochemistry. 1998; 35:2117–2128. [PubMed: 8652554]
35. Bujalowski W, Jezewska MJ. Thermodynamic Analysis of the Structure-Function Relationship in the Total DNA-Binding Site of Enzyme - DNA Complexes. Meth Enzym. 2009; 466:294–324.
36. Bujalowski W, Jezewska MJ. Macromolecular competition titration method: Accessing Thermodynamics of the Unmodified Macromolecule-Ligand Interactions Through Spectroscopic Titrations of Fluorescent analogs. Meth Enzym. 2011; 488:17–57. [PubMed: 21195223]
37. Bujalowski W, Klonowska MM. Negative Cooperativity in the Binding of Nucleotides to *Escherichia coli* Replicative Helicase DnaB Protein. Interactions with Fluorescent Nucleotide Analogs. Biochemistry. 1993; 32:5888–5900. [PubMed: 8504109]
38. Galletto R, Rajendran S, Bujalowski W. Interactions of Nucleotide Cofactors with the *Escherichia coli* Replication Factor DnaC Protein. Biochemistry. 2000; 39:12959–12969. [PubMed: 11041861]
39. Galletto R, Jezewska MJ, Bujalowski W. Interactions of the *E. coli* DnaB Helicase Hexamer with the Replication Factor the DnaC Protein. Effect of Nucleotide Cofactors and the ssDNA on

Protein-Protein Interactions and the Topology of the Complex. J Mol Biol. 2003; 329:441–465. [PubMed: 12767828]

40. Marcinowicz A, Jezewska MJ, Bujalowski W. Multiple Global Conformational States of the Hexameric RepA Helicase of Plasmid RSF1010 With Different ssDNA-Binding Capabilities Are Induced By Different Numbers of Bound Nucleotides. Analytical Ultracentrifugation and Dynamic Light Scattering Studies. J Mol Biol. 2008; 375:386–408. [PubMed: 18022636]
41. Bujalowski W, Klonowska MM, Jezewska MJ. Oligomeric Structure of *Escherichia coli* Primary Replicative Helicase DnaB Protein. J Biol Chem. 1994; 269:31350–31358. [PubMed: 7989299]
42. Roychowdhury A, Szymanski MR, Jezewska MJ, Bujalowski W. Interactions of the *E. coli* DnaB - DnaC Protein Complex With Nucleotide Cofactors. 1 Allosteric Conformational Transitions of the Complex. Biochemistry. 2009; 48:6712–6729. [PubMed: 19569622]
43. Roychowdhury A, Szymanski MR, Jezewska MJ, Bujalowski W. Mechanism of NTP Hydrolysis by the *Escherichia coli* Primary Replicative Helicase DnaB Protein. 2 Nucleotide and Nucleic Acid Specificities. Biochemistry. 2009; 48:6730–6746. [PubMed: 19435286]
44. Jezewska MJ, Bujalowski W. Global Conformational Transitions in *E. coli* Primary Replicative DnaB Protein Induced by ATP, ADP and Single-Stranded DNA Binding. J Biol Chem. 1996; 271:4261–4265. [PubMed: 8626772]
45. Cantor, RC.; Schimmel, PR. Biophysical Chemistry. Vol. II. W. H. Freeman; New York: 1980. p. 591-641.
46. Williams KR, Konigsberg WH. Identification of Amino Acid Residues at Interface of Protein-Nucleic Acid Complexes by Photochemical Cross-Linking. Meth Enzym. 1991; 208:516–539. [PubMed: 1779846]
47. Sambrook, J.; Fritsch, EF.; Maniatis, T. Molecular Cloning Laboratory Manual. Vol. 1. C.S.H., Laboratory Press; 1989. p. 6.39
48. Jezewska MJ, Kim US, Bujalowski W. Binding of *Escherichia coli* Primary Replicative Helicase DnaB Protein to Single-Stranded DNA. Long-Range Allosteric Conformational Changes Within the Protein Hexamer. Biochemistry. 1996; 35:2129–2145. [PubMed: 8652555]
49. Jezewska MJ, Marcinowicz A, Lucius AL, Bujalowski W. DNA Polymerase X from African Swine Fever Virus. Quantitative Analysis of the Enzyme – ssDNA Interactions and the Functional Structure of the Complex. J Mol Biol. 2006; 356:121–41. [PubMed: 16337650]
50. Jezewska MJ, Galletto R, Bujalowski W. Interactions of the RepA helicase hexamer of plasmid RSF1010 with the ssDNA. Quantitative Analysis of Stoichiometries, Intrinsic Affinities, Cooperativities, and Heterogeneity of the Total ssDNA-Binding Site. J Mol Biol. 2004; 343:115–136. [PubMed: 15381424]
51. Epstein IR. Cooperative and Non-cooperative Binding of Large Ligands to a finite One-Dimensional Lattice. A Model For Ligand - Oligonucleotide Interactions. Biophys Chem. 1978; 8:327–339. [PubMed: 728537]
52. Hill, TL. Cooperativity Theory in Biochemistry. Steady State and Equilibrium Systems. Springer-Verlag; New York: 1985. p. 167-2340.
53. Bujalowski W, Lohman TM, Anderson CF. On the Cooperative Binding of Large Ligands to a One-Dimensional Homogeneous Lattice: The Generalized Three-State Lattice Model. Biopolymers. 1989; 28:1637–1643. [PubMed: 2775853]
54. Record MT, Lohman TM, deHaseth PL. Ion Effects on Ligand - Nucleic acid Interactions. J Mol Biol. 1976; 107:145–158. [PubMed: 1003464]
55. Record MT, Anderson CF, Lohman TM. Thermodynamic Analysis of Ion Effects on the Binding and Conformational Equilibria of Proteins and Nucleic Acids: the Roles of Ion Association or Release, Screening, and Ion Effects on Water Activity. Quart Rev Biophys. 1978; 11:103–178.
56. Lohman TM, Bjorson KP. Mechanisms of Helicase-Catalyzed DNA Unwinding. Annu Rev Biochem. 1996; 65:169–214. [PubMed: 8811178]
57. Delagoutte E, von Hippel PH. Helicase Mechanisms and the Coupling of Helicases Within Macromolecular Machines. Part II: Integration of Helicases into Cellular Processes. Q Rev Biophys. 2003; 36:1–69. [PubMed: 12643042]

58. Szymanski MR, Jezewska MJ, Bujalowski W. Binding of Two PriA - PriB Complexes to the Primosome Assembly Site Initiates the Primosome Formation. J Mol Biol. 2011; 411:123–142. [PubMed: 21641914]

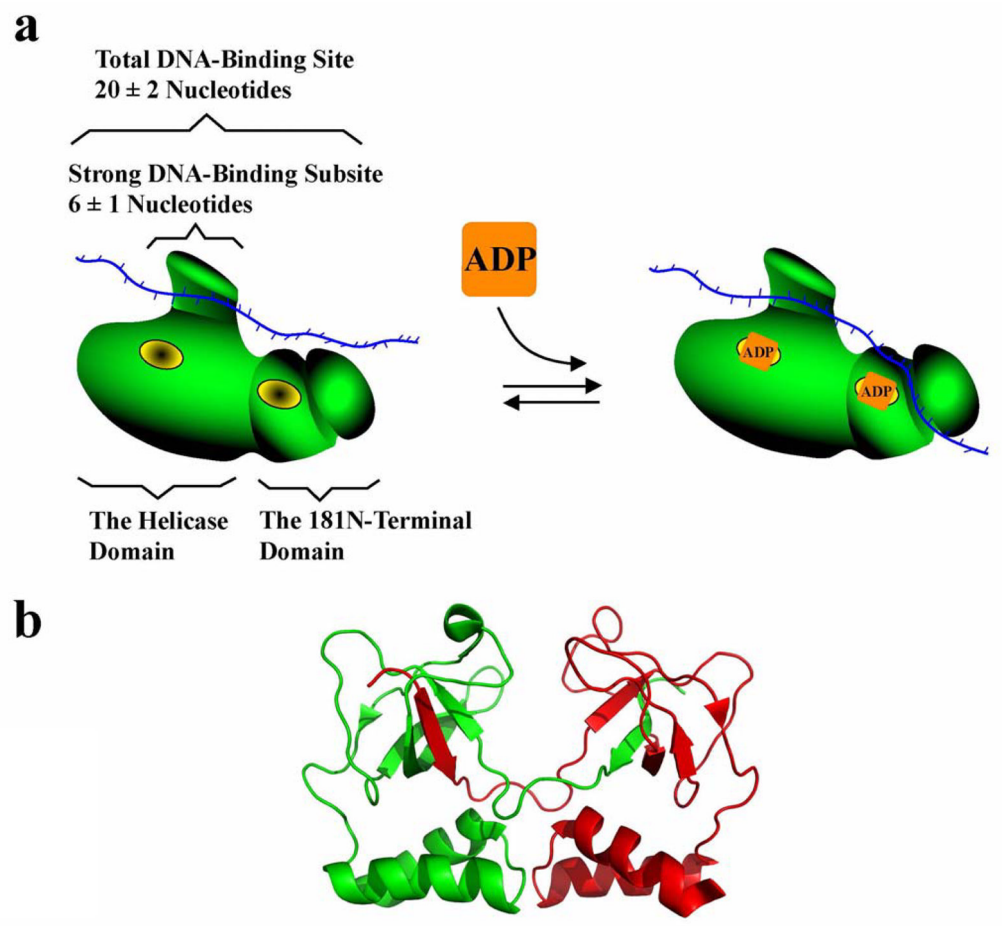

Figure 1.

a. Schematic model of the PriA helicase in the complex with the ssDNA and ADP (15–17,19–23). The enzyme has two domains, two nucleic acid binding subsites, and two nucleotide-binding sites (15–17,19–23). The total site-size of the enzyme - ssDNA complex is ~20 nucleotides. The strong DNA-binding subsite of the enzyme on the helicase domain occludes ~6 nucleotides. The 181N-terminal domain of the protein also contains the DNA-binding-subsite (21). The yellow ovals symbolize the strong and weak nucleotide-binding sites of the helicase, although their location, with respect to protein domains, *prior* to this work, was arbitrary assigned (21). In the absence of nucleotide cofactors, only the strong subsite on the helicase domain engages the nucleic acid. Upon binding ADP to both nucleotide-binding sites, the DNA-binding subsite of the helicase on the N-terminal domain opens and enters into interactions with the ssDNA (21). **b**. Structure of the 105N-terminal subdomain dimer of the PriA helicase, based on crystallographic data (18). The structure has been generated using data from Brookhaven Protein Data Bank, under the code 2D7E using PyMOL (DeLAno Scientific, San Carlos, CA). Each monomer is marked in a different color.

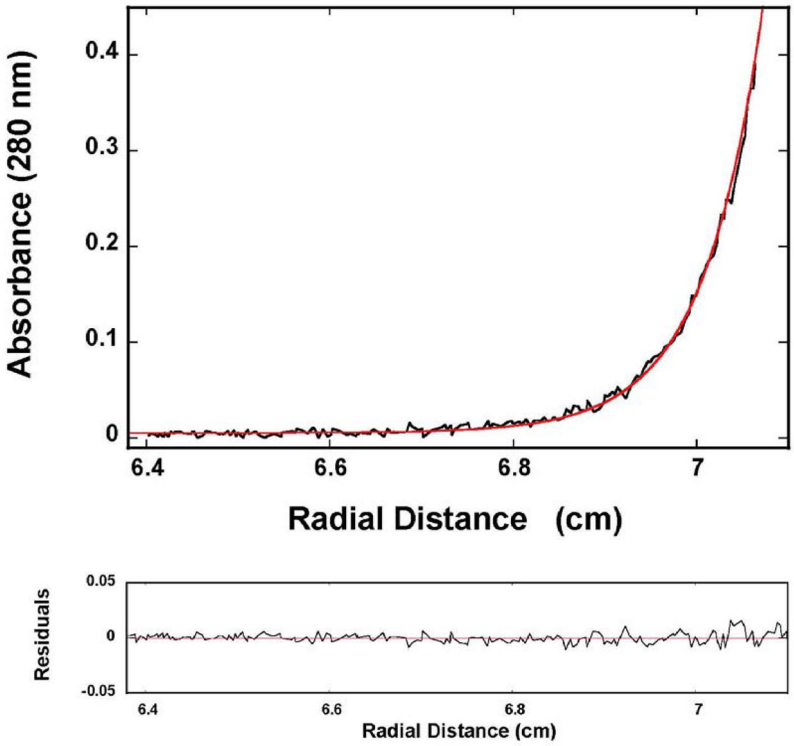

Figure 2.

Sedimentation equilibrium concentration profiles of the 181N-terminal domain of the *E. coli* PriA in buffer C (pH 7.0, 10°C). The concentration of the protein is 5.98×10^{-6} M (monomer). The profile has been recorded at 280 nm and at 24,000 rpm. The solid line is the nonlinear least-squares fit to a single exponential function (eq. 2), with a single species having a molecular weight of 41,000 ± 3000. Lower panel shows the residuals of the fit.

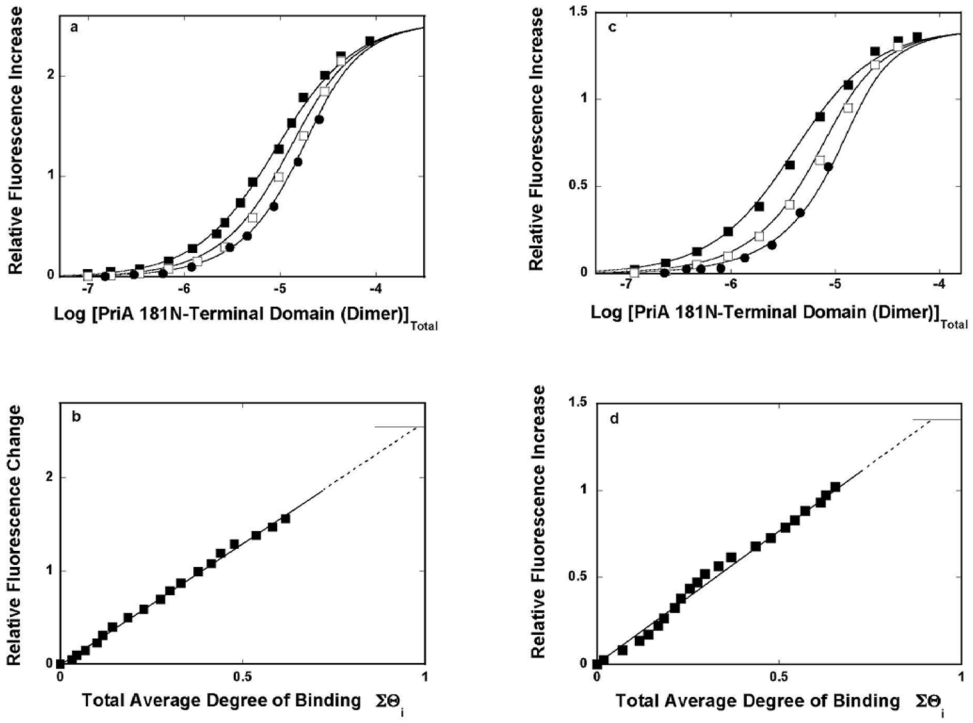

Figure 3.

a. Fluorescence titrations (λ_{ex} = 325 nm, λ_{em} = 410 nm) of the ssDNA 12-mer, dεA(pεA)$_{11}$, with the 181N-terminal domain of the PriA helicase in buffer C (pH 7.0, 10°C), at three different concentrations of the nucleic acid: (■) 1.76×10^{-6} M, (❑) 8.78×10^{-6} M, and (●) 1.76×10^{-5} M. The solid lines are nonlinear least-squares fits of the fluorescence titration curves according to the one-site binding model defined by eq. 3 (details in text). **b.** The dependence of the relative fluorescence increase, ΔF, upon the total average degree of binding, $\Sigma\Theta_i$, of the 181N-terminal domain dimer - 12-mer complex. The values of $\Sigma\Theta_i$ have been determined using the quantitative method outlined in Materials & Methods. The solid straight line follows the data points and does not have theoretical basis. The dashed straight line is an extrapolation of the total average degree of binding to the maximum value of the observed fluorescence increase $\Delta F_{max} = 2.54 \pm 0.1$ that provides the maximum stoichiometry of 0.98 ± 0.15 of the domain dimer - oligomer complex. **c.** Fluorescence titrations of the ssDNA 24-mer, dεA(pεA)$_{23}$, substrate with the 181N-terminal domain of the PriA helicase in buffer C (pH 7.0, 10°C) at three different concentrations of the nucleic acid: (■) 1.5×10^{-6} M, (❑) 7.5×10^{-6} M, and (●) 1.5×10^{-6} M. The solid lines are nonlinear least-squares fits of the fluorescence titration curves according to the one-site binding model defined by eq. 3 (details in text). **d.** The dependence of the relative fluorescence increase, ΔF, upon $\Sigma\Theta_i$ of the 181N-terminal domain dimer - 24-mer complex. The solid straight line follows the data points and has no theoretical basis. The dashed line is an extrapolation of $\Sigma\Theta_i$ to the maximum value of the observed fluorescence increase, $\Delta F_{max} = 1.41 \pm 0.11$, that provides the maximum stoichiometry of 0.92 ± 0.14 of the domain dimer - 24-mer complex.

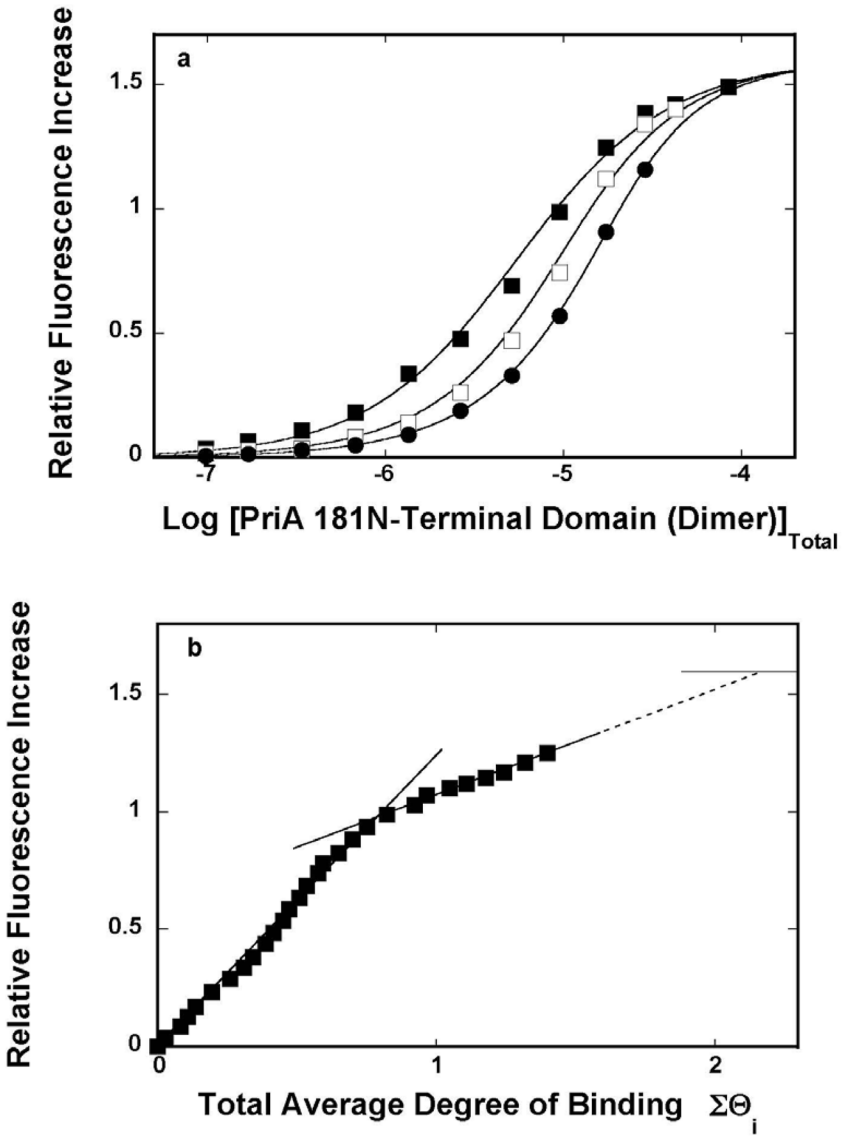

Figure 4.

a. Fluorescence titrations (λ_{ex} = 325 nm, λ_{em} = 410 nm) of the ssDNA 26-mer, dεA(pεA)$_{25}$, with the 181N-terminal domain of the PriA helicase in buffer C (pH 7.0, 10°C), at three different concentrations of the nucleic acid: (■) 1.76×10^{-6} M, (❑) 8.78×10^{-6} M, and (●) 1.76×10^{-5} M. The solid lines are nonlinear least-square fits of the fluorescence titration curves according to the two-sites binding model, defined by eqs. 6 – 9 (details in text). **b.** The dependence of the relative fluorescence increase, ΔF, upon the total average degree of binding, $\Sigma\Theta_i$, of the 181N-terminal domain dimer - 26-mer complex. The solid straight lines are the limiting slopes of the high and low-affinity binding phases. The dashed straight line is an extrapolation of the low affinity phase part of the plot to the maximum value of the observed fluorescence increase $\Delta F_{max} = 1.6 \pm 0.1$ that provides the maximum stoichiometry of 2.2 ± 0.2 of the domain dimer - 26-mer complex (details in text).

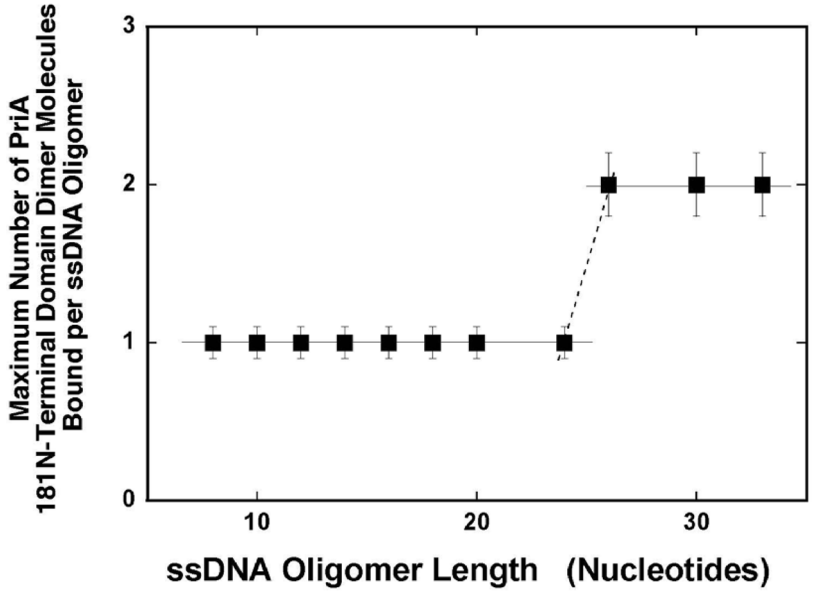

Figure 5.

The maximum stoichiometry of the 181N-terminal domain dimer on the ssDNA oligomer as a function of the length of the oligomer (nucleotides). The solid horizontal lines connect the points with the same maximum stoichiometry. The dashed line marks the transition of the maximum stoichiometry from one dimer molecule to two dimer molecules per the ssDNA oligomer.

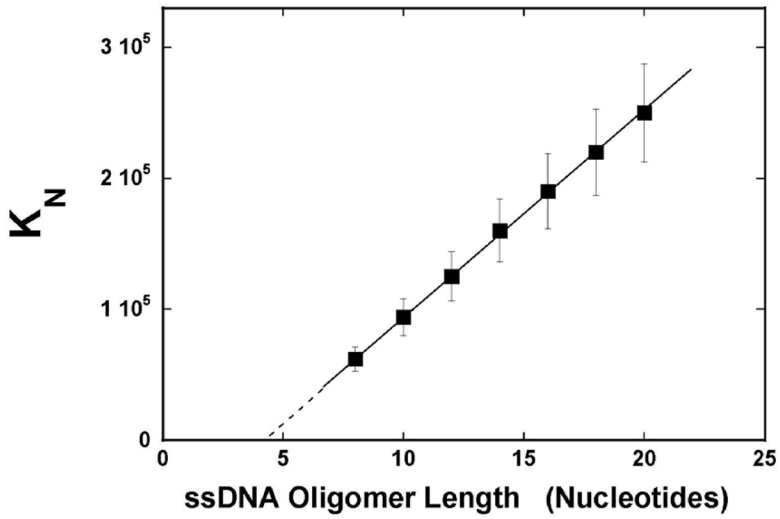

Figure 6.

The dependence of the macroscopic, equilibrium binding constant, K_N, characterizing the binding of the 181N-terminal domain dimer to different etheno-derivatives of the ssDNA oligomers, which accept only a single domain dimer, upon the length of the ssDNA oligomer (nucleotides). The solid line is the linear least-squares fit of the plot according to eqs. 4 and 5. The dashed line is the extrapolation of the plot to the zero value of the macroscopic equilibrium binding constant.

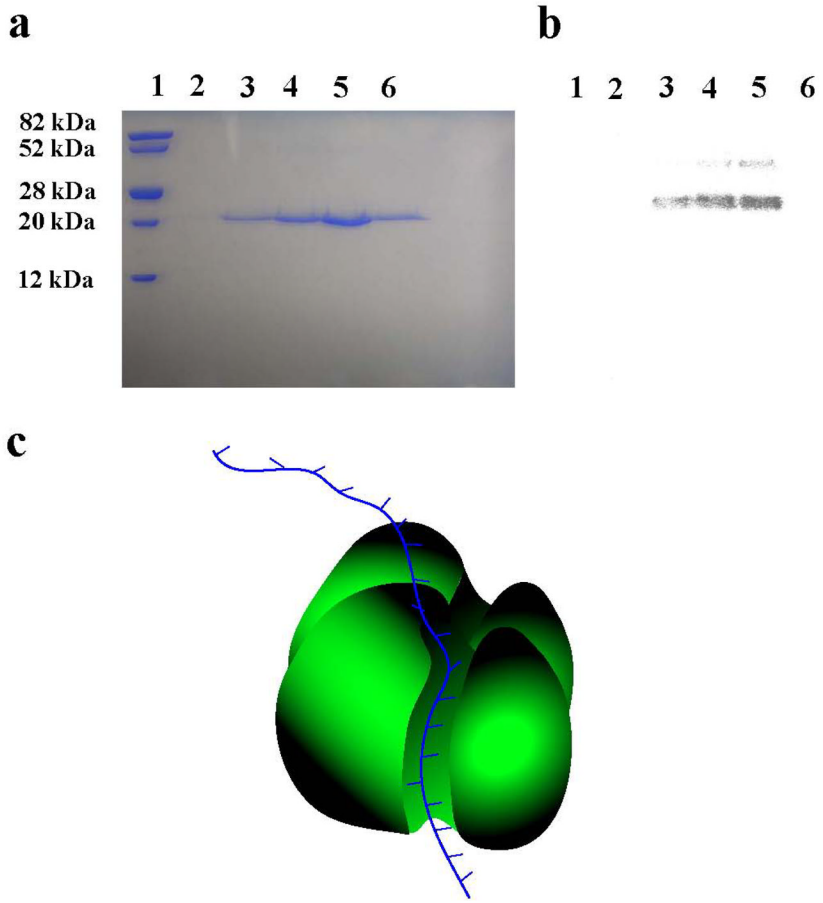

Figure 7.

a. The 15% SDS polyacrylamide gel of the 181N-terminal domain - [^{32}P]-dT$_{20}$ complex, after UV-mediated cross-linking of the protein to the DNA, formed at different concentrations of the domain dimer, in buffer C (pH 7.0, 10°C) and stained with Coomassie Brilliant Blue (Materials and Methods). The concentration of the [^{32}P]-dT$_{20}$ is 3×10^{-7} M (oligomer). Lane 1 contains protein markers. Lane 2 contains [^{32}P]-dT$_{20}$ alone. Lanes 3 to 5 contain the constant concentration of the ssDNA 20-mer and the increasing concentration of the domain (dimer): lane 3, 3×10^{-6} M; lane 4, 6×10^{-6} M; and lane 5, 9.0×10^{-6} M. Lane 6 contains only the 181N-terminal domain (3×10^{-6} M (dimer)) in the absence of the [^{32}P]-dT$_{20}$. **b**. The autoradiogram of the same SDS polyacrylamide gel, as shown in panel a. **c**. Schematic model of the 181N-terminal domain dimer - ssDNA complex (details in text).

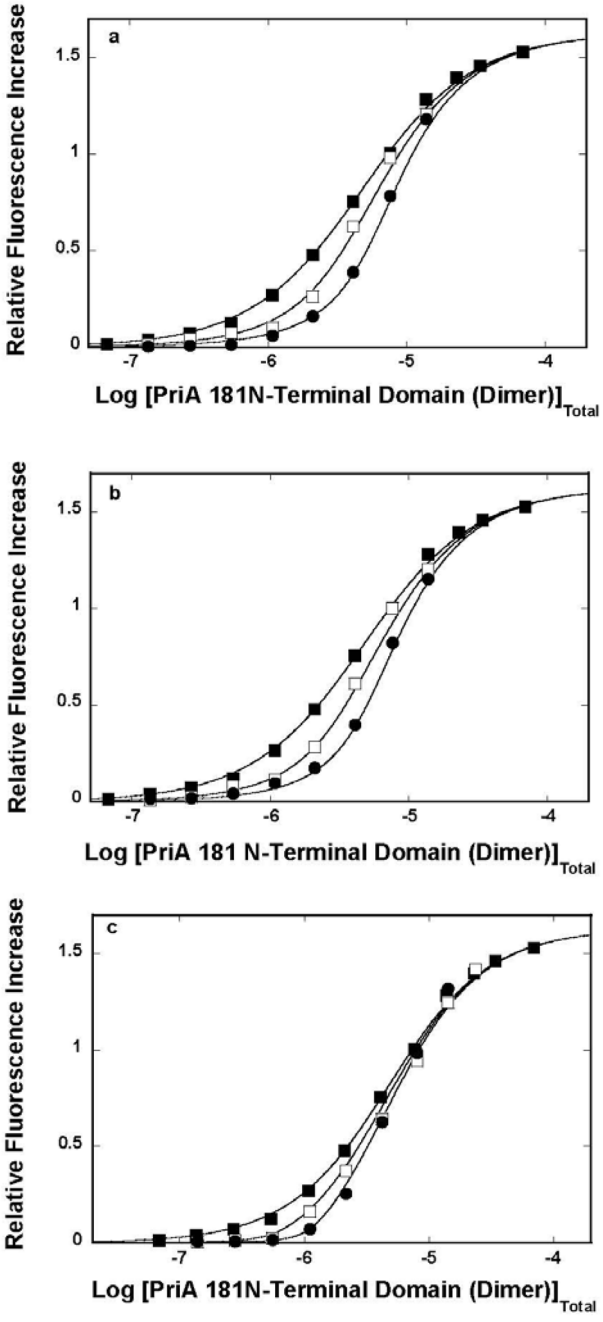

Figure 8.

a. Fluorescence titrations of the ssDNA 20-mer, dεA(pεA)$_{19}$, with the 181N-terminal domain (λ_{ex} = 325 nm, λ_{em} = 410 nm) in buffer C (pH 7.0, 10°C) in the absence (■) and presence of two different concentrations of dT(pT)$_{19}$, 1.74 × 10^{-6} M (❑) and 4.16 × 10^{-6} M (λ) (oligomer), respectively. **b.** Fluorescence titrations of the ssDNA 20-mer, dεA(pεA)$_{19}$, with the 181N-terminal domain (λ_{ex} = 325 nm, λ_{em} = 410 nm) in buffer C (pH 7.0, 10°C) in the absence (■) and presence of two different concentrations of dC(pC)$_{18}$pCp, 1.71 × 10^{-6} M (❑) and 3.73 × 10^{-6} M (λ) (oligomer). **c.** Fluorescence titrations of the ssDNA 20-mer, dεA(pεA)$_{19}$, with the 181N-terminal domain (λ_{ex} = 325 nm, λ_{em} = 410 nm) in buffer C (pH 7.0, 10°C) in the absence (■) and presence of two different concentrations of dsDNA 10-mer

(Materials & Methods). The concentrations of the dsDNA 10-mer are: 5.0×10^{-7} M (❑) and 1.0×10^{-6} M (λ) (oligomer), respectively. In all panels, the concentration of dεA(pεA)$_{19}$, is 1.43×10^{-6} M (oligomer). The solid lines in all panels are nonlinear least-squares fits of the titration curves using eqs. 10 – 12, with the binding $K_N = 1.7 \times 10^6$ M^{-1} and $\Delta F_{max} = 1.18$ for dεA(pεA)$_{19}$. The binding constants for the examined nucleic acids are included in Table 2.

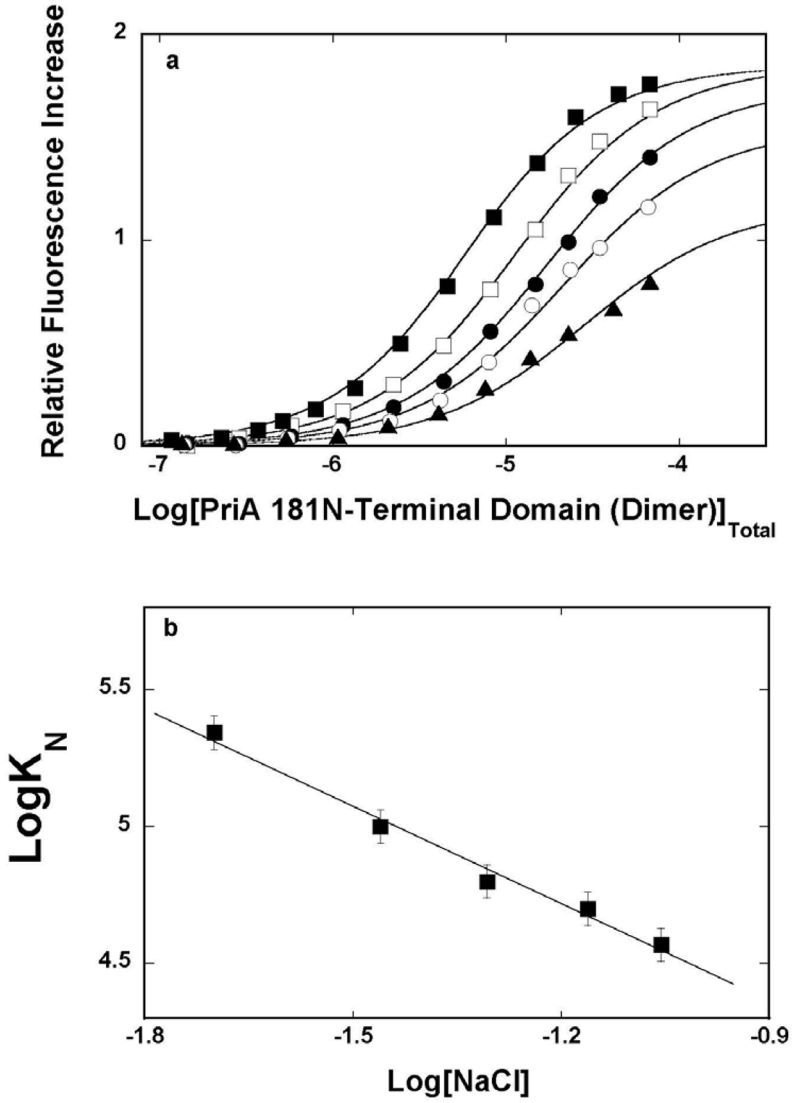

Figure 9.

a. Fluorescence titrations of the ssDNA 18-mer, dεA(pεA)$_{17}$, with the 181N-terminal domain (λ_{ex} = 325 nm, λ_{em} = 410 nm) in buffer C (pH 7.0, 10°C), containing different NaCl concentrations: 20 mM (■), 34.7 mM (❑), 49.4 mM (●), 69 mM (❍), and 89 mM (λ). The concentration of the ssDNA 18-mer is 2.43 × 10^{-6} M (oligomer). The solid lines are nonlinear least-squares fits of the titration curves, using eq. 3, with ΔF_{max} and K_N: 1.85, 2.2 × 10^5 M^{-1} (■); 1.85, 1 × 10^5 M^{-1} (❑); 1.75, 6.3 × 10^4 M^{-1} (●); 1.55, 5 × 10^4 M^{-1} (❍); 1.17, 3.7 × 10^4 M^{-1} (σ). **b.** The dependence of the logarithm of the binding constant, K_N, upon the logarithm of [NaCl]. The solid line is the linear least-squares fit, which provides the slope, $\partial \mathrm{Log}K_N/\partial \mathrm{Log}[\mathrm{NaCl}] = -1.2 \pm 0.3$.

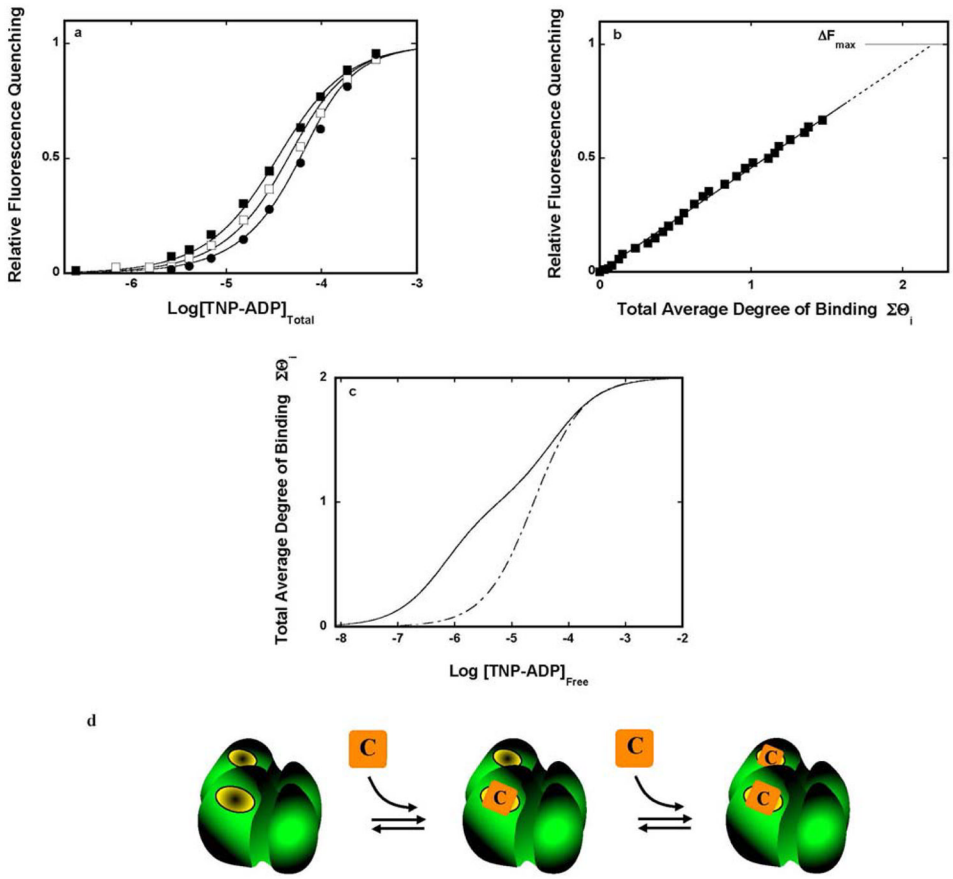

Figure 10.

a. Fluorescence titrations of the 181N-terminal domain with TNP-ADP in buffer C (pH 7.0, 10°C) at different protein concentrations (dimer): 9.85×10^{-6}M (■), 2.0×10^{-5} M (❑), 3.5×10^{-5} M (●). The solid lines are nonlinear least-squares fits of the titration curves, according to the model of two different, discrete and cooperative binding sites (eqs. 13 – 15), using a single set of binding parameters: $K_{C1} = K_{C2} = 4.1 \times 10^4$ M^{-1}, σ =1, and ΔF_{max} = 1.0. **b.** Dependence of the relative fluorescence quenching, ΔF, upon the average degree of binding of TNP-ADP on the 181N-terminal domain dimer, $\Sigma\Theta_i$, (■). The values of $\Sigma\Theta_i$ have been determined using the quantitative method described in Materials & Methods. The solid line follows the experimental points and has no theoretical basis. The dashed line is an extrapolation of $\Sigma\Theta_i$ to the maximum value of the fluorescence quenching, ΔF_{max} (details in text). **c**. The dependence of the total average degree of binding of TNP-ADP on the intact PriA helicase (solid line) and on the 181N-terminal domain dimer as a function of the free cofactor concentration. The plots were generated using the binding parameters for the intact enzyme and the for the domain dimer, respectively (details in text). **d**. Schematic representation of the nucleotide cofactor, C, binding to the 181N-terminal domain dimer.

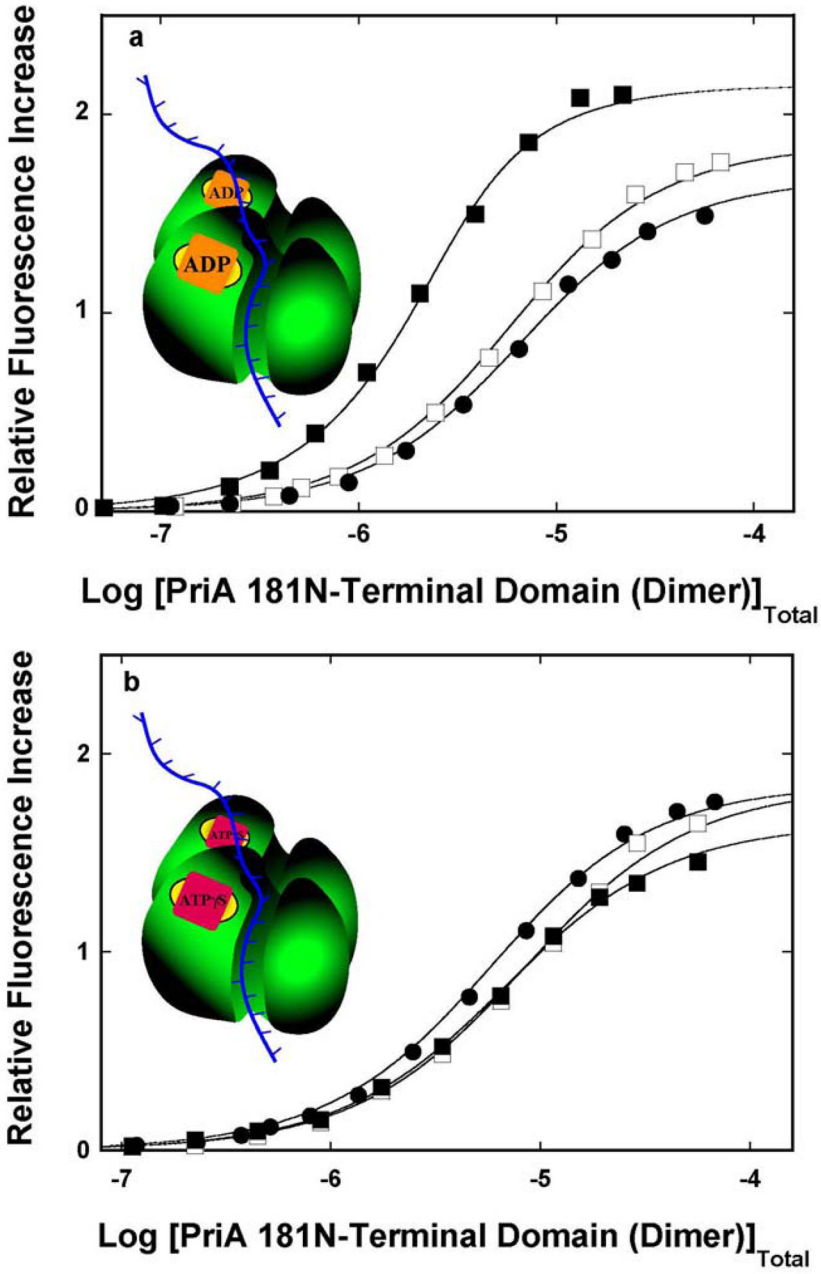

Figure 11.

a. Fluorescence titrations of the ssDNA 18-mer, dεA(pεA)$_{17}$, with the 181N-terminal domain (λ_{ex} = 325 nm, λ_{em} = 410 nm) in buffer C (pH 7.0, 10°C), in the absence (❑) and presence of different ADP concentrations: 1×10^{-5} M (●); 3×10^{-3} M (■). The concentration of the ssDNA 18-mer is 2.43×10^{-6} M (oligomer). The solid lines are nonlinear least-squares fits of the titration curves, using eq. 3, with ΔF_{max} and K_N: 1.85, 2.2 × 105 M^{-1} (❑); 1.68, 1.9×10^5 M^{-1} (●); 2.15, 1.2×10^6 M^{-1} (■). **b.** Fluorescence titrations of the ssDNA 18-mer, dεA(pεA)$_{17}$, with the 181N-terminal domain (λ_{ex} = 325 nm, λ_{em} = 410 nm) in buffer C (pH 7.0, 10°C), in the absence (❑) and presence of different ATPγS concentrations: 1×10^{-4} M (●) and 3×10^{-3} M (■), respectively. The concentration of the ssDNA 18-mer is 2.43×10^{-6} M (oligomer). The solid lines are nonlinear least-squares fits

of the titration curves, using eq. 3, with ΔF_{max} and K_N: 1.85, 2.2×10^5 M^{-1} (❑); 1.84, 1.4×10^5 M^{-1} (●); 1.65, 1.8×10^6 M^{-1} (■). Inserts schematically show the final tertiary complexes of the examined association processes in the presence of a saturating concentration of the corresponding nucleotide cofactor.

Table 1

Thermodynamic and spectroscopic parameters characterizing the binding of the *E. coli* PriA helicase 181N-terminal domain to etheno-derivatives of ssDNA oligomers in buffer C (pH 7.0, 10°C) (details in text)*.

	8-mer	10-mer	12-mer	14-mer	16-mer	18-mer	20-mer	24-mer	26-mer	30-mer	33-mer
n	1 ± 0.1	1 ± 0.1	1 ± 0.1	1 ± 0.1	1 ± 0.2	1 ± 0.2	1 ± 0.2	1 ± 0.2	2 ± 0.2	2 ± 0.2	2 ± 0.2
K_N (M^{-1})	(6.2 ± 0.9) × 10^4	(9.4 ± 1.7) × 10^4	(1.3 ± 0.2) × 10^5	(1. 6 ± 0.3) × 10^5	(1. 9 ± 0.3) × 10^5	(2.2 ± 0.4) × 10^5	(2.5 ± 0.4) × 10^5	(3.1 ± 0.5) × 10^5	-	-	-
K_i (M^{-1})	(1.6 ± 0.3) × 10^4	(1.6 ± 0.3) × 10^4	(1.9 ± 0.3) × 10^4	(1.6 ± 0.3) × 10^4	(1.6 ± 0.3) × 10^4	(1.6 ± 0.3) × 10^4	(1.6 ± 0.3) × 10^4	(1.6 ± 0.3) × 10^4	(2.0 ± 0.4) × 10^4	(2.0 ± 0.4) × 10^4	(1.5 ± 0.3) × 10^4
ω	-	-	-	-	-	-	-	-	27 ± 8	28 ± 9	20 ± 7
ΔF_1	-	-	-	-	-	-	-	-	1.25 ± 0.05	0.80 ± 0.05	0.65 ± 0.05
ΔF_{max}	3.10 ± 0.10	2.33 ± 0.05	2.55 ± 0.05	1.95 ± 0.05	1.23 ± 0.05	1.83 ± 0.05	1.15 ± 0.05	1.41 ± 0.05	1.60 ± 0.05	1.45 ± 0.05	1.33 ± 0.05

*The errors are standard deviations determined using 3 – 4 independent titration experiments.

Table 2

Macroscopic and intrinsic binding constants, K_N and K_{in}, and the site-size, n, characterizing the binding of the PriA helicase 181N-terminal domain to different ssDNA homo-oligomers, $dN(pN)_{19}$, homo-oligomer, $dC(pC)_{18}pCp$, containing phosphate group; at the 3′-end, and the dsDNA 10-mer, in buffer C (pH 7.0, 10°C). The values of the binding constants for the unmodified nucleic acids have been determined using the MCT Method (details in text)*.

	$d\varepsilon A(p\varepsilon A)_{19}$	**$dA(pA)_{19}$**	**$dT(pT)_{19}$**	**$dC(pC)_{19}$**	**$dC(pC)_{18}pCp$**	**dsDNA 10-mer**
K_N (M^{-1})	$(2.5 \pm 0.4) \times 10^5$	$(1.3 \pm 0.4) \times 10^6$	$(1.5 \pm 0.4) \times 10^6$	$(4.5 \pm 0.8) \times 10^6$	$(1.6 \pm 0.3) \times 10^6$	$(3.0 \pm 1.0) \times 10^7$
K_{in} (M^{-1})	$(1.6 \pm 0.3) \times 10^4$	$(8.1 \pm 0.2) \times 10^4$	$(9.4 \pm 0.2) \times 10^4$	$(2.8 \pm 0.5) \times 10^5$	$(1.0 \pm 0.2) \times 10^5$	-
p**	5	5	5	5	5	-

* Errors are standard deviations determined using 3–4 independent titration experiments.

** The site-size of the strong DNA-binding subsite (details in text).